THE EFFECT OF NANOPARTICLES ADDITION ON THE PROPERTIES OF POLYURETHANE

By

VISHANTH UPPU

Bachelor of Engineering in Mechanical Engineering

Osmania University

Hyderabad, Telangana, India

2014

Submitted to the Faculty of the
Graduate College of the
Oklahoma State University
in partial fulfillment of
the requirements for
the Degree of
MASTER OF SCIENCE
May, 2018

THE EFFECT OF NANOPARTICLES ADDITION ON

THE PROPERTIES OF POLYURETHANE

Thesis Approved:

Dr. Ranji Vaidyanathan

Thesis Adviser

Dr. Pankaj Sarin

Dr. James Smay

ACKNOWLEDGEMENTS

The happiness and the excitement that accompany the successful completion of thesis would be incomplete without the mention of people who made it possible. First and foremost, I avail this opportunity to express my gratitude to my advisor Dr. Ranji Vaidyanathan for providing a chance to pursue a Master of Science degree at Oklahoma State University and allowing me to conduct research in his lab. His constant support and endless guidance has helped me in accomplishing all the tasks. He always had faith in me and inspired me in many ways. I am grateful to him for everything he has given to me.

I would like to thank Dr. Pankaj Sarin and Dr. James Smay for accepting my request and being in my thesis committee. They had been very helpful, and I always received their valuable suggestions, whenever needed.

I wholeheartedly thank Tinesha Vallejo, Matt Villarreal, Efren Luevano and all other employees at Infinite Composite Technologies, Tulsa for the help and support they had given me throughout my study. I extend this opportunity to thank Oklahoma Center for Advancement of Science and Technology (OCAST) for funding this research under Project No. AR16-032.

I am extremely thankful to my fellow graduate students and friends, Ragini, Bindu, Dilli, Vishal, Ravi, Muthu, Ranjan, Shamim, Padmanapan, Malay, Swathi for their advices and valuable time. I must thank Dr. Mishra for the help and guidance whenever I approached.

I am always thankful to my family and friends for their love and support throughout my life.

Name: VISHANTH UPPU

Date of Degree: MAY, 2018

Title of Study: THE EFFECT OF NANOPARTICLES ADDITION ON THE PROPERTIES OF POLYURETHANE

Major Field: MATERIALS SCIENCE AND ENGINEERING

Abstract: This research is aimed at analyzing the properties of polyurethane nanocomposites, before and after cryogenic exposure. Graphene and Cloisite 30B were chosen as filler materials and the main purpose of adding these fillers is to improve the barrier properties. Clay was added to the hard segment while the graphene was added to the soft segment of polyurethane matrix. The nanocomposites with single-additive and with dual-additives were prepared by incorporating different concentrations of graphene and clay into polyurethane. These samples were then characterized using DSC, DMA and SEM. Instron machine was utilized to measure the tensile properties. The focus was on comparing the influence of using one-additive and two-additives on polyurethane and investigating the degradation of the nanocomposites due to initial cryogenic exposure. The results indicated that the uniform dispersion of the fillers led to an increase in glass transition temperature, stiffness and tensile modulus of the composites while the agglomeration at higher loadings decreased these properties. When exposed to cryogenic temperatures, micro-cracks were seen in samples with higher loadings of clay while there was no considerable change noticed in all the properties denoting the suitability of polyurethane composites for cryogenic applications. To assess the gas permeability characteristics of the composites an instrument was designed adhering to standard test method documented in ASTM D-1434(15).

TABLE OF CONTENTS

Chapter Page

LIST OF TABLES

Table Page

LIST OF FIGURES

Figure Page

CHAPTER I

INTRODUCTION

In the recent years, composite materials have attracted a lot of researchers all over the world in the field of engineering. Though the use of traditional materials still exists, the developments in material science and the designs of components demands considering alternative materials. Composite materials provide good strength to weight ratios, low cost, improved thermal and mechanical properties and many other desirable aspects depending on the application. Among myriad applications of composite materials like aircraft and naval structures, automobiles, medical devices, etc., their use in low temperature fuel tanks could result in an increase in the efficiency of the system.

Lightweight and strong composite materials are already in use for many space applications such as vehicle launch bodies, fairings and payload components. In the vehicles that go into the space, the size may not matter but the weight of each component and cost of the project does matter. It costs approximately $9000/lb to transport payload into the space[1]. Therefore, every ounce saved will directly help in reducing the project costs. There has been extensive research going on at National Aeronautics and Space Administration (NASA) to develop a cost-effective launch system since 2002 [2]. One primary consideration to reduce the weight in these vehicles would be to use light weight fuel tanks. The tank systems to store super cool liquid fuels like liquid oxygen, liquid hydrogen and liquid nitrogen are still dominated by metals. The regular tanks that store cryogenic

liquids use multiple layers of insulators and metal liners. The weight and cost of the metal liner would directly influence on the total weight and cost of these tanks. A potential composite liner would be a good alternative to these metal liners. So, the research trend on investigating the cryogenic properties of different composite materials not only to use them as liners but also to gain the advantages like light weight and low cost in fabricating a composite fuel tank has grown in the past few years.

In addition to the cryogenic fuels for space applications, the use of Liquefied Natural Gas (LNG) in place of existing fuels has also gained importance in the past few years for environmental concerns and to save potential fuel gas. It is well known that more amount of fuel can be stored in the liquefied state which is an advantage for long-haul on-highway busses and class 8 trucks or semis. LNG can provide longer driving ranges per refueling because it only takes up about $1/600^{th}$ of the volume that Compressed Natural Gas (CNG) occupies at room temperature and atmospheric pressure [3]. The LNG storage tanks that are commercially available in the market are very heavy, complex and expensive. The initial type of tank system is a Dewar type consisting of a stainless-steel tank disposed inside of a further steel tank with vacuum between the two tanks and it can be maintained at a low pressure (about 150 psi). The disadvantage of this type of tank is it need a pumping assembly to maintain the vacuum between two steel tanks. Therefore, there is also a need in manufacturing a light weight and low-cost all composite tank to store LNG.

The growth and demand for these light weight and low-cost composite fuel tanks lead to various improvements and modifications. The evolution of the tanks designed to store and hold liquids and gases under pressure has proceeded through four distinct stages: all-metal tanks (Type I), metal hoop-wrapped composite tanks (Type II), metal-lined composite tanks (Type III) and plastic-lined composite tanks (Type IV). The fifth stage, an all-composite, liner-less Type V tank has been the pressure vessel industry's Holy Grail for years [4].

A Composite Overwrapped Pressure Vessel (COPV) was developed in the year 2012 by NASA with the help of Boeing to store cryogenic liquids [5]. A small tank with diameter of 2.4 meters was initially tested at NASA Marshal Space Flight Centre followed by a 5.5 meters diameter tank, which was the largest composite tank ever built. These tanks are very well established with a metal liner overwrapped with continuous fiber/matrix system. The main purpose of metal liner is to minimize permeation and thermal stresses at very low temperatures. However, the mismatch in coefficient of thermal expansion between metal liner and other layers on the tank and embrittlement of liner results in microcracking and delamination [6]. The most commonly used metal liners in Type III tanks are Aluminum and stainless steel, while some other metal alloys are also studied extensively. Type IV tanks use a polymer liner which can be produced by extrusion, injection molding, roto-molding or blow molding. Several polymers were investigated as liner materials, High density Polyethylene (HDPE), Polyamide (PA), Liquid crystal Polymer (LCP) are some them. These liners are then overwrapped with fiber-resin systems using filament winding technique. Though, these tanks generated considerable weight savings, the manufacturing cost is roughly twice that of their predecessors. Therefore, to minimize the costs and reduce the weight further, there is need in designing an unlined or liner-less composite tank which can sustain test conditions and maintain structural integrity.

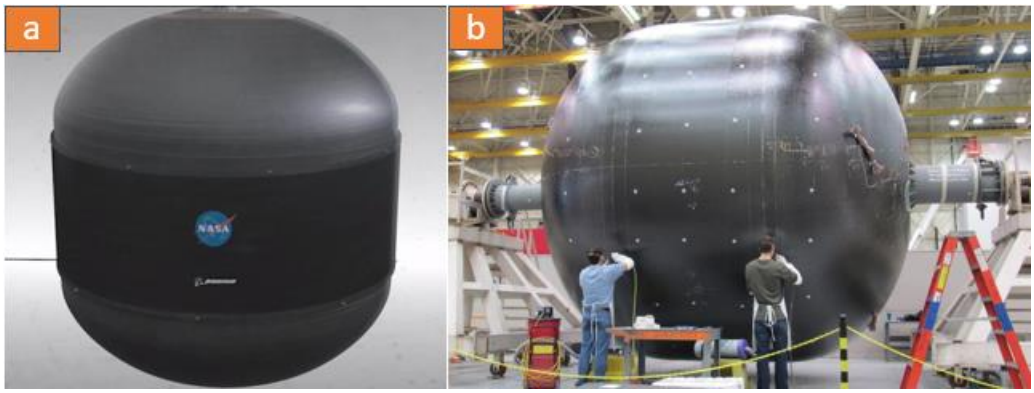

Figure 1 Composite Cryogenic Tanks deveoped by NASA and BOEING a) 2.4m diameter tank b) 5.5m diameter tank.

This research is initiated to develop a potential polymer composite material system that can be used in designing a liner-less all composite tank for the storage of low temperature, pressurized fuels. The tanks are fabricated using a washable water-soluble tooling material on a filament winder to avoid the liner and use multiple layers of different materials and composites to sustain the cryogenic conditions. The polymer should possess a wide variety of properties to be considered as a suitable material for this application. Low glass transition temperature (T_g), low Coefficient of Thermal Expansion (CTE), excellent bonding and adhesive nature, good barrier properties, impact resistant, ability to use as a coating are some of the important parameters.

The possibility of using polyurethane and its nanocomposites as cryogenic tank material has been discussed in this work. The properties of the composites before and after cryogenic exposure are investigated and reported.

1.1 Polyurethane (PU)

Polyurethane is the widely used Polymer material which bridges the gap between rubber and plastics [7]. Any polymer consisting of urethane linkage (-NHCOO-) as major repeating unit are called Polyurethanes. It was first developed as an alternative to rubber during world war II, since then it has gained lot of importance all over the world because of its unique chemistry, suitability and versatility which led to its incorporation in wide range of applications such as biomedical, building and construction, aerospace, automotive and textiles [8-11].

Polyurethanes (PU) are formed by a rapid interaction of a diisocyanate and a polyol/diamine component. The resulting polymer is considered as a segmented co-block polymer containing alternate hard (diisocyanate) and soft segments (polyol/diamine). The glass transition temperature of soft segment (SS) is generally below room temperature while that of hard segment (HS) is above room temperature. Due to hydrogen bonding and rigidity, PU self-assembles into a continuous rubbery matrix with dispersed rigid domains which are very well connected to the rubbery phase

through physical cross-links and have nano-scale dimensions representing an ideal filler polymer composite. The phase separated morphology is generally observed in PU due to thermodynamic incompatibility of HS and SS [11].

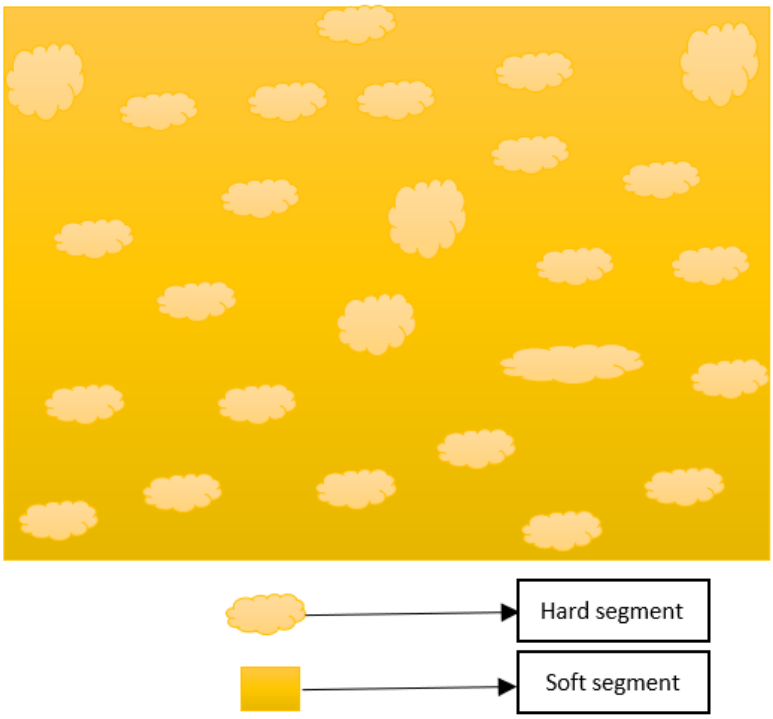

Figure 2 Schematic diagram of Hard segment and Soft segment in PU.

Polyurethanes can be synthesized in different ways which group them into several different classes based on their form and desired properties. They occur in the form of rigid, semi rigid, flexible foams, thermoplastic, binders, coatings, adhesives, sealants and elastomers[12]. The growth of industries and the ability to combine the durability and toughness of metals with the elasticity of rubber of this material made it to use in several engineered products. North America Polyurethane market was valued at USD 12.09 billion in 2015 [13]. United States Polyurethane market revenue by product from 2010 to 2024 is shown in the figure 3.

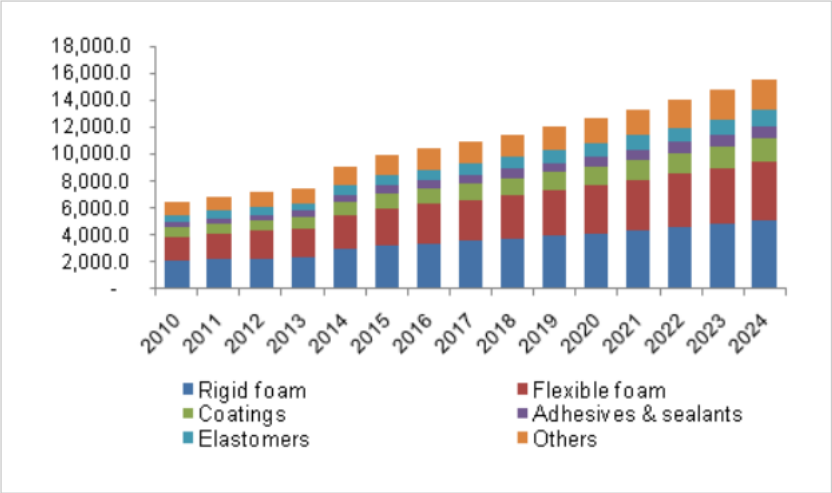

Figure 3 United States Polyurethane products Market revenue adapted from [13].

The existence in different forms of polyurethane has attracted many industries especially coating industries. There is a growing range of applications and advantageous markets that may be derived from the use of PUs as coatings as they offer very good mechanical, chemical and physical properties [14]. High chemical resistivity, excellent drying, low temperature flexibility, adequate scratch resistivity and good adhesion properties of PU has made it suitable for the coating application [12,15]. The global market share of Polyurethane coatings in 2011 excluding architectural paints can be estimated nearly to 15%. The polyurethane coatings are grouped into six different types in ASTM D16 Standard[16]. Types I, II, III and VI are one package polyurethanes while types IV and V are two package polyurethanes. Most high solids and solvent-less PU coatings for high performance application and corrosion protection are designed using two package type V polyurethane coating which is obtained from reacting an isocyanate rich component with a polyol or diamine.

Though polyurethane has many advantages when compared with the other polymers, there is always a need to alter its properties for desired application. Polymer matrix materials become brittle at cryogenic temperatures. The toughness and other crucial properties of PU suppressed at these temperatures can be retained or improved by adding various modifying agents. In addition to this,

material should act as a barrier for boil-off of cryogenic fluids. The barrier properties can be improved by creating a tortuous diffusion path using nano-additives. Therefore, reinforcement materials such as carbon nano tubes, carbon black, glass fiber, graphene, nano clay and several other fillers are currently used in the industries to meet the end requirements. The selection of the modifier depends on factors like working temperatures, curing time, quality of dispersion, cost and availability. Graphene nanoplatelets and Cloisite 30B are the two additives that are used in this research work.

1.2 Graphene Nanoplatelets

Graphene is an allotrope of carbon element which was first isolated by simple mechanical exfoliation in 2004 [17]. It is a two-dimensional honey comb single layer crystal lattice formed by the tightly packed sp^2 bonded carbon atoms. Due to the unique structure of graphene, it exhibits better electrical, mechanical, physical and optical properties [18]. Additional factors such as their availability in nature, cost-effectiveness, high specific surface area, which carries higher levels of transferring stress across interface provides higher reinforcement [19]. These nanoplatelets possess isotropic electrical/thermal conductivities in the graphene plane, low viscosity and non-toxicity when compounded with polymer. All these properties of graphene have encouraged researchers to consider them as reinforcing agents with Polyurethane.

Moreover, graphene polymer composites have been used extensively as coatings [18]. Polyurethane Acrylate coating electrical conductivity was enhanced by adding graphene. The increase in graphene content has also led to better mechanical properties [20].

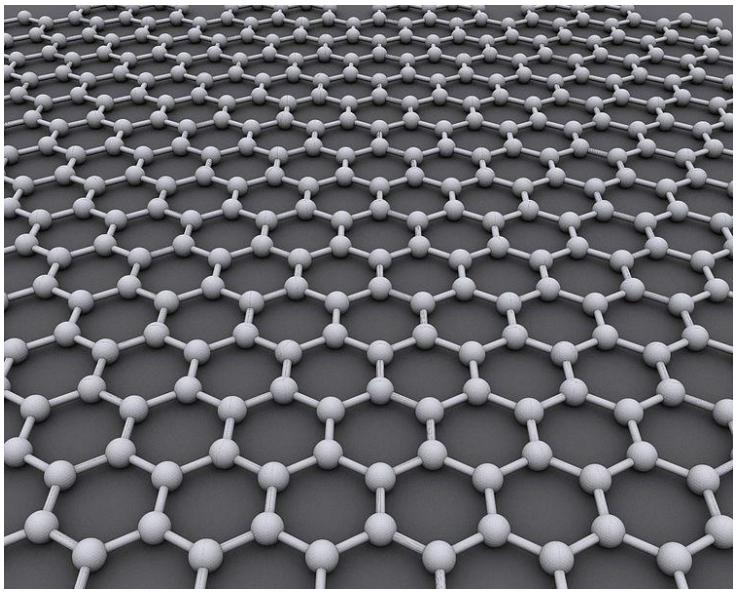

Figure 4 The ideal crystalline structure of graphene adapted from [21]

1.3 Cloisite 30B

There are many articles in the literature which discussed about the polymer nanocomposites prepared by addition of organoclays formed from montmorillonite[22, 23]. Clay has been used significantly in altering the gas barrier properties of polymer nanocomposites [24, 25]. The main consideration to improve the barrier properties is the homogenous dispersion of these nano-particles into polymer matrix to create a tortuous diffusion pathway[26, 27]. The richest intercalation chemistry of clay is an added advantage along with all the superior properties. The only disadvantage of clay is the incompatibility between the hydrophilic clay and hydrophobic polymer causing agglomeration[28]. To overcome this, surface modification of clay is implemented using cationic exchange reaction. In this reaction, Na^{+} and Ca^{2+} residing in interlayer regions of clay particles are replaced by organic cations to render hydrophilic silicate to organophilic and creating good compatibility with polymer matrix resulting in homogenous dispersion. The organophilization reduces the energy of the clay and is key step for successful exfoliation of clay particles into polymer matrix [29]. Cloisite 30B is such kind of a modified clay in which Methyl, tallow, bis-2-hydroxy ethyl, ammonium is used as a modifier.

1.4 Hypothesis

1. The presence of graphene and clay layers in between the PU matrix would alter the molecular motions and improve the glass transition temperature.
2. The uniform dispersion of clay and graphene in the matrix wouldn't induce microcracks when exposed to low temperatures unlike fibers.
3. The incorporation of two different fillers would improve the modulus better when compared with the individual filler at a similar concentration.
4. The initial cryogenic exposure for 2 hours may not degrade thermal and mechanical properties significantly.

1.5 Literature Review

The behavior of polymer composite materials at cryogenic temperatures has been studied to a large extent [30]. However, the use of composite materials for cryogenic fuel tanks is not clearly understood. The earlier work has mainly focused on thermal cycling of unidirectional composites and their damage behavior and permeability under fatigue thermal loads [31-33]. Bechel et al. [34] studied the stacking effect on microcracking in a cryogenically cycled carbon-bismaleimide composite and observed that there is a linear relationship between microcrack density and number of times submerged in LN_2 and investigated the trade-off between higher service temperature and lower microcrack resistance. Their group has also worked on the permeability calculations for composite at cryogenic temperatures and reported that maximum temperature applied on the composite can also affect the lowest temperature it can sustain [35]. In addition to this, many articles were published discussing about the leakage of the gases through composite laminates at cryogenic conditions [36-40].

The new developments in manufacturing a liner-less composite tank was started in the year 2005. Kaushik Mallick et al. with the aid of Air Force Research laboratory, Kirtland, USA, have described a way to improve the design and capabilities of lightweight liner-less composite tanks[41]. The considerations for fabricating prototype tanks such as material development and characterization, micromechanics-based analysis and the structural design are explained. Epoxy was toughened to improve the resistance to microcrack formation using rubbers and block copolymer impact modifiers. Vapor grown carbon fibers were also used as reinforcements for the matrix to improve modulus and interlaminar shear strength. They have described an approach to develop composite materials that can meet the requirements for a potential tank material.

M.d. Islam et al. researched on woven composites with and without cryogenic exposure[42]. The influence of cryogenic exposure on the mechanical properties of woven composites using Kevlar and Carbon fibers as reinforcements were reported. It was observed that there is no considerable change (less than 5%) in both Kevlar and Carbon laminates tensile strength and tensile chord modulus even after 6 hours of cryogenic exposure. The flexural strength and flexural chord modulus for both the composites also remained unaltered when compared with pristine material response. The inter laminar shear strength of Kevlar fiber composite has reduced by 16.8% while it was not changed much with Carbon fibers. The microscopic images of the composites indicated that there was no growth of cracks even after cryogenic exposure.

Xiao Jun Shen et al.[43] studied the reinforcing effect of graphene on the properties of epoxy resins at cryogenic temperature. The introduction of graphene into epoxy matrix has enhanced its properties at both room temperature and cryogenic temperature. It was seen that the tensile strength was improved by 17.1% with only 0.1wt% graphene, but further addition of graphene decreased the strength because of agglomeration. The interfacial bonding between the graphene and epoxy was observed to be better at 77K than at RT due to the thermal shrinkage of epoxy at 77K. The other mechanical properties also improved by addition of graphene. Enhancing the properties at

RT and 77K by addition of very low content of graphene indicated that it is the best suitable filler material at cryogenic temperatures. His group also reported the improvement in interlaminar shear strength of glass fabric/epoxy composites by adding graphene oxide[44].

Yi-He Zhang et al. investigated the cryogenic properties of polyimide-MMT nanocomposites [45]. The addition of MMT at low contents (1-3wt%) enhanced the mechanical properties both at RT and 77K and proved to be a suitable insulating material at cryogenic temperatures. But at higher loading of 20wt%, tensile strength and modulus at 77K decreased because of the agglomerations of MMT which acted as stress concentrations. At 77K, the elongation at break of the composite was larger for low (1-5wt%) of MMT than at 10wt%. The reduction in mechanical properties at 77K for higher loadings of MMT is mainly because of the aggregation and cracking at the interface.

Jiao-Ping Yang et al. has reported the behavior of Epoxy-MMT Nanocomposites at Cryogenic temperature[46]. The incorporation of MMT at 1wt% increased the glass transition temperature form 107^0C to 111^0C while for 2wt% and 3wt% it decreased. This may be due to the low mobility of polymer chains and interruptions in crosslinking of epoxy at higher loadings. The tensile strength was found to be higher at 77K than RT for all the samples and the maximum strength was achieved with 1wt% MMT while the lowest value was with 3wt%. This might be because of the pullout of agglomerated MMT creating micro-sized holes and acting as crack initiators resulting in failure. The tensile modulus increased with increase in MMT content at RT and 77K while the notched impact strength decreased at 77K with increase in filler.

Sandi G. Miller et al.[47] developed polymer layered silicate composites for cryo-tank applications. Epoxy 826 was chosen as matrix material and cloisite 30B as the nano filler. The permeability of the nanocomposites decreased when compared with neat sample. However, an increase in permeability was seen after cryogenic cycling of these nanocomposites when compared with uncycled samples. Microcracking was not observed after cycling, but a change in glass transition

temperature was due to change in free volume resulting from repeated temperature change. They have also developed two kinds of Epoxy nanocomposites by using different hardeners, one glassy at RT and the other rubbery at RT. The rubbery nanocomposites toughness was increased more than 100% by addition of cloisite 30B while it was decreased in the glassy nanocomposites. The CTE was reduced by 30% by addition of nano clay as it inhibits polymer chain motion for the glassy blend, but it has shown no effect on the CTE of rubbery blend. The oxygen permeability of rubbery samples was much higher due to greater polymer chain mobility.

Many research works were performed on improving the properties of polyurethane using various nano-additives at room temperature. But, there is no sufficient information reported on its properties at cryogenic temperatures or after exposing to cryogenic temperatures.

M.M Gudarzi et al. incorporated self-aligned graphene sheets into PU matrix and reported the improvement in electrical and mechanical properties of PU [48]. They developed a new latex mixing method to produce graphene reinforced PU composites. These nano-composites containing uniformly dispersed and highly oriented graphene sheets with strong bonding with PU exhibited increase in hardness, tensile modulus and strength, electrical conductivity at very low filler loading. Dongyu Cai et al. [49]disclosed that graphene oxide nanoplatelets reinforced PU has shown significant improvements in modulus and hardness of the composites. Enhancement in anti-scratch and barrier properties were reported which are key requirements for surface coatings. The decrease in tensile strength was because of the destruction of hard segments by the two-dimensional graphene sheets.

S.K.Yadav et al. [50] has worked on enhancing the properties of polyurethane using functionalized graphene nanoplatelets. The addition of graphene provided considerable improvement in mechanical and thermal properties of PU. At 2wt% loading, modulus increased by ten times whereas thermal stability was shown 30^0C higher than pure PU. Hyunwoo Kim et al. [51] has

worked on improving gas barrier properties of polyurethane composites using graphene. At 3wt% loading, 80%-90% reduction in nitrogen permeability was reported. The graphene was seen to be an excellent material to enhance the properties of polyurethane.

Nano Clay has also proven to be a suitable filler material for polymers. Rehnama et al. [52] has investigated the effect of different nano clays on PU properties. It was observed that among all the clays, cloisite 30B has shown better mechanical and thermal properties. It is because of the compatibility of cloisite 30B with PU matrix leading to good exfoliation. Xia Cao et al. [53] has also reported that better dispersion of cloisite 30B was achieved by pre-mixing it with isocyanate component. Pattanayak and Jana [54-56] have also reported their studies on polyurethane and cloisite 30B nanocomposites.

1.6 Objectives

In the literature, polyurethane composites were prepared by using either graphene or cloisite 30B as reinforcing agents. As discussed earlier, polyurethane is a two-phase component. This research is focused on assessing the properties of polyurethane composites with different modifying agents in each phase of polyurethane. Cloisite 30B is added to hard segment while graphene is added to the soft segment and the dispersion of these additives is achieved by utilizing a high-speed shear mixer, avoiding the use of solvents. The two main objectives of this research work are

- To develop single-additive and dual-additives PU composites using graphene and cloisite 30B as fillers.
- To improve the thermal and mechanical properties of the composites at room temperature and analyzing the effect of cryogenic exposure for 2 hours on the properties of polyurethane composites.

The thermal and mechanical properties of the composites are measured before and after cryogenic exposure. The low temperature exposure is to estimate the suitability of polyurethane as a material for cryogenic tank applications.

CHAPTER II

MATERIALS AND METHODOLOGY

2.1 Materials

The two-part Polyurethane system was purchased from BJB Enterprises, USA. One Part considered as Part-A is Aromatic diisocyanate (hard segment) and the other part is considered as Part-B is Oligomeric diamine (soft segment). The two parts A and B are mixed in a weight ratio of 1:5 as suggested by the manufacturer. The graphene nanoplatelets dispersion in Part-B was obtained from Applied Graphene Materials, USA. Nano clay Cloisite 30B was supplied by Southern Clay Products, USA. Silicone Material which was used to make the molds was also purchased from BJB Enterprises.

2.2 Preparation of Nanocomposites

The mixing of two parts and addition of nano additives to these parts was achieved by using a high-speed shear mixer from Flacktek inc., USA. All the components are degassed before using. For the composites that have only graphene, the calculated amount of graphene dispersion was first added to part B and mixed at 1500 rpm for 10 minutes. Part-A was added to the above blend and allowed to mix for 10 minutes at 1500 rpm. The final mixture was then kept in vacuum to minimize air bubbles and poured onto the molds to get thin sheets.

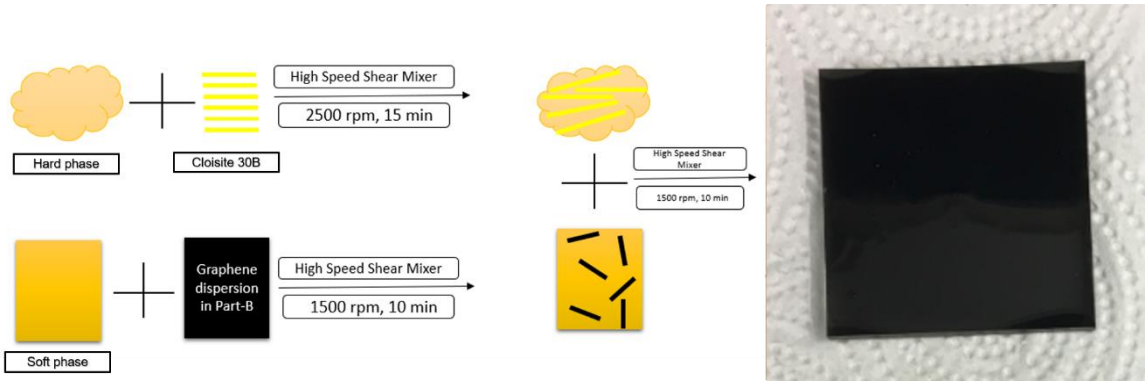

Figure 5 Schematic representation of sample preparation.

The specimens with clay are prepared by adding the required amount of Cloisite 30B to the hard segment and mixing it at 2500 rpm for 15 minutes followed by addition of soft segment and mixing for another 10 minutes at 1500 rpm. The mixture is then placed in vacuum to minimize air bubbles, poured onto the molds and allowed to cure at room temperature for 24 hours before testing.

The dual-additive composites are prepared in similar method. Cloisite 30B is added to hard segment and mixed for 15 minutes at 2500 rpm. Required amount of graphene dispersion is added to soft phase and mixed at 1500 rpm for 10 minutes. These two blends are then combined at a speed of 1500 rpm for 10 minutes followed by vacuum and curing at room temperature.

2.3 Differential Scanning Calorimetry (DSC)

DSC is one of the effective ways to measure the glass transition temperature of polymers. The analysis was carried out using a DSC Q2000 from TA Instruments, USA. The samples were cut, weighed between 5-10 mg and loaded into aluminum pans which are then crimped with a lid. Aluminum pans and lids were obtained from DSC Consumables, Inc. Three samples of each compositions were measured, and the standard deviation was calculated. Each sample was subjected to three thermal cycles. Initially sample was cooled down to -90^0C and maintained isothermal for 5 minutes. In all the cycles sample was kept isothermal for 5 minutes at the final temperatures. The first cycle was heating the sample at a rate of 10^0C/min from -90^0C to 150^0C. This step is to erase the thermal history of the sample. The second cycle was cooling down from

150^0C to -90^0C at 10^0C/min. The final cycle was to re-heat the sample from -90^0C to 150^0C at 10^0C/min. The step change in heat flow for the third cycle was considered as glass transition temperature. The tests were conducted on all the samples before and after cryogenic exposure.

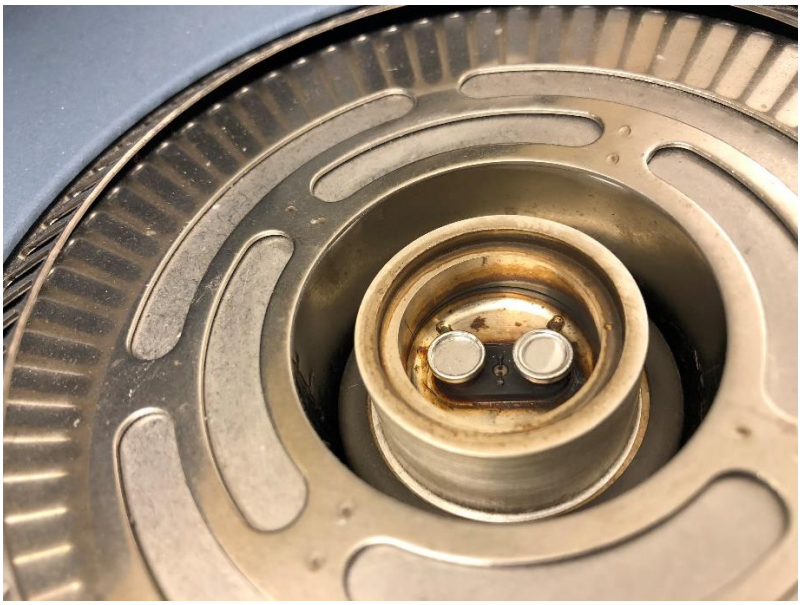

Figure 6 DSC Furnace with reference pan and sample

2.4 Scanning Electron Microscopy (SEM)

SEM was used to study the surface morphology of the nanocomposites. The fractured surfaces of the samples were gold coated for 30 seconds and loaded into the chamber of SEM. A FEI Quanta 600 FEG ESEM was utilized with accelerating voltage of 15KV. This analysis was carried out to understand the dispersion of graphene and clay with PU matrix and the agglomeration of these nano-additives at higher loadings. The samples were dipped in liquid nitrogen and the fractured surfaces of these samples are investigated for micro-cracks that may develop due to the cryogenic exposure.

2.5 Dynamic Mechanical Analysis (DMA)

The thermal-mechanical properties of the polyurethane and its composites are investigated using a DMA Q800 from TA Instruments and liquid nitrogen was used as gas cooling accessory. This analysis was carried out to examine the viscoelastic properties of the polyurethane and its composites. The stress-strain responses at different temperatures was also observed. The tests were conducted on a tensile clamp with the specimen dimensions approximately 1mm thick, 18mm long and 5.5mm width in the temperature range of -100^0C to 50^0C. Ramping rate was 3^0C/min, frequency of 1Hz and an amplitude of 10µm was set for all the experiments.

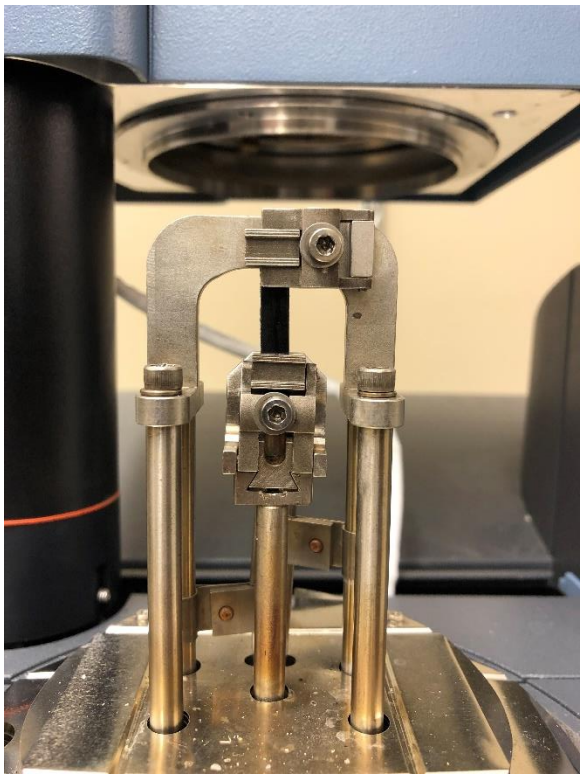

Figure 7 Tensile loading of the sample in DMA

2.6 Tensile Testing

The tensile testing of the composite specimens was performed on Instron 5567, according to ASTM standard D638. The samples are prepared by following the dimensions listed for reinforced composites and a speed of 20 in./min was set for all the tests. A mold negative was designed, machined and silicone molds were made using the negative. A set of 5 samples were tested for each composition before and after the cryogenic exposure.

Figure 8 Mold negative and silicone mold used to prepare samples for tensile testing on Instron

Figure 9 Tensile testing on Instron

2.7 Permeability Measurement Set-up

An instrument was designed to measure the gas permeability of the composites adhering to ASTM Standard D1434. The sample is loaded into a gas transmission cell to form a sealed semi barrier between two chambers. One chamber contains the test gas at a specific pressure and the other chamber can either be evacuated or maintained at atmospheric pressure. If one chamber is evacuated, transmission of gas through specimen is indicated by an increase in pressure, if it is maintained at atmospheric pressure transmission of gas is indicated by a change in volume.

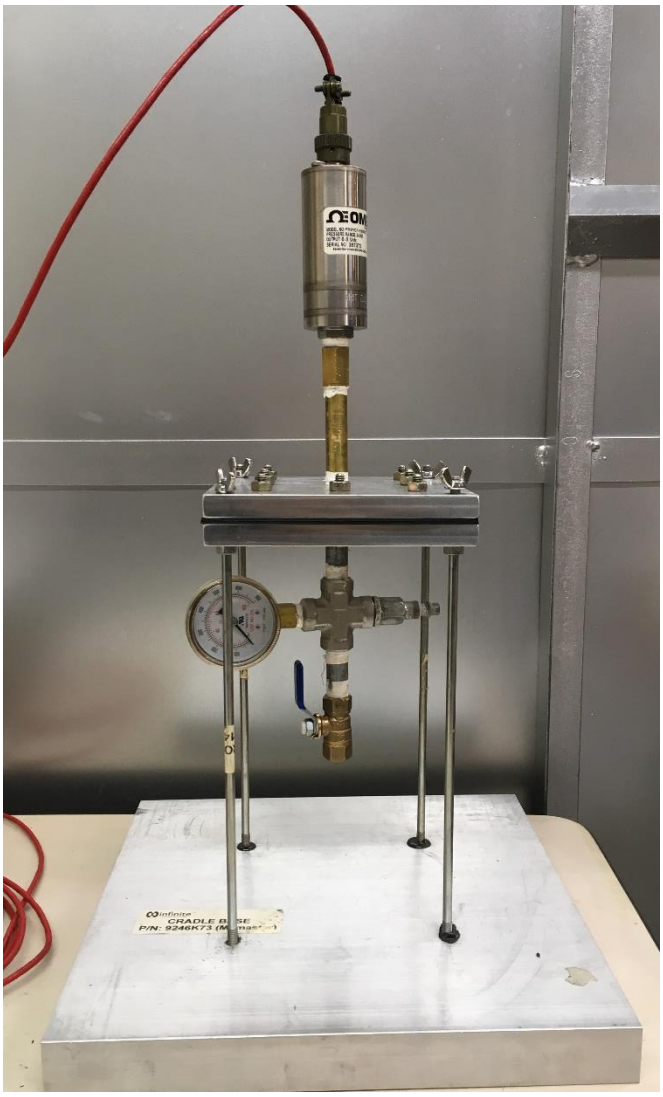

Figure 10 Permeability measurement set-up

CHAPTER III

RESULTS AND DISCUSSIONS

3.1 Glass Transition Temperature (T_g)

The glass transition temperature of polyurethane and its nanocomposites is analyzed using DSC. The results shown in below figures emphasize on variation in glass transition temperature (obtained from second heating cycle) for different fillers and at different loadings. It can be observed that there is an increase in T_g by the addition of fillers. This is because T_g is function of rotational freedom and anything that restricts rotation would increase the T_g. In the nanocomposite, good dispersion of graphene and clay could lead to substantial interphase zone altering the mobility of polymer chains. The movability of polyurethane molecules was reduced by incorporation of nano-additives with larger surface area resulting in an increase in glass transition temperature. The increase in T_g with an increase in filler concentration can be seen because, more the fillers, more the inhibition in segmental and fictional motions in PU chains which eventually leads to a higher T_g value. The addition of 0.5wt% of clay and graphene has shown no considerable change in T_g whereas the 1wt% of graphene and clay raised the T_g value more than 1^0C.

In the dual-additive composites, an increase of more than 3^0C in T_g was noticed. In these composites, molecular motions in hard phase are restricted by clay while in the soft phase are restricted by graphene. This could have altered the mobility of the molecules in whole matrix more when compared with single-additive composites.

Glass transition temperature is also used in evaluating the flexibility in a polymer. In addition to chain flexibility, the molecular weight, crosslinking and intermolecular attractions are some important factors which effect T_g. As the chain becomes more flexible, the polymer molecules can move at lower temperatures corresponding to a lower T_g. The addition of clay at high weight (%)

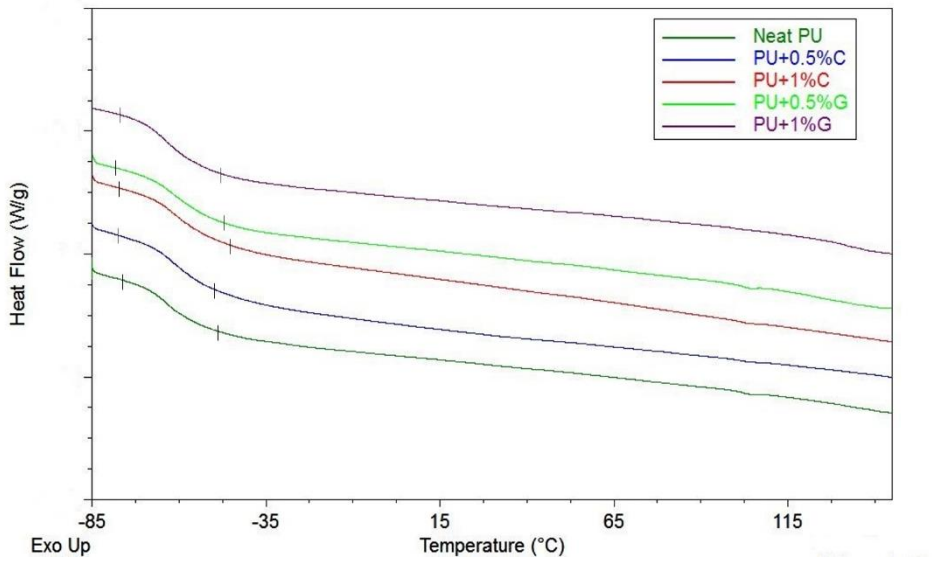

Figure 11 DSC plot of single-additive PU composites

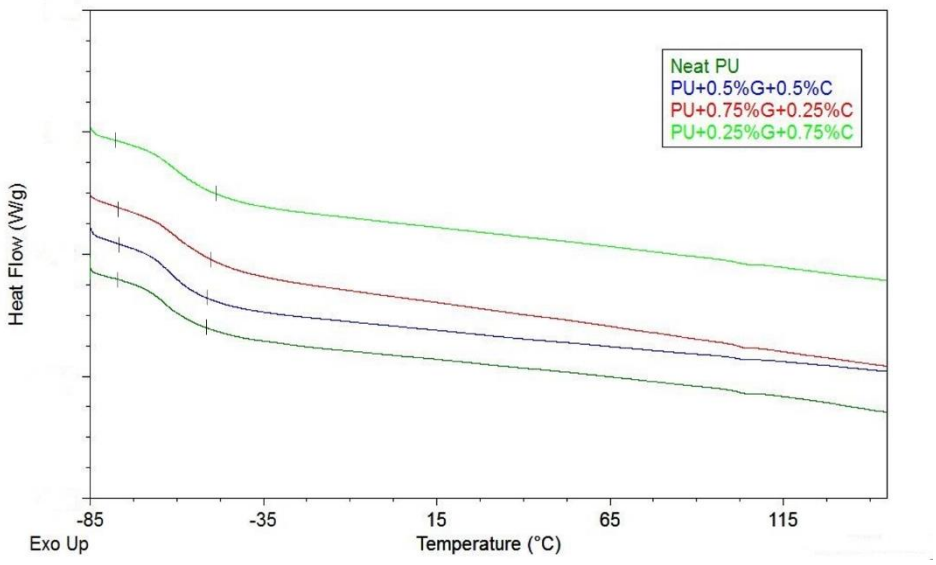

Figure 12 DSC plot of dual-additive PU composites at 1wt%.

such as 5wt% has shown a decrease in glass transition temperature. This might be because of the formation of clay agglomerates and interruption of these agglomerates in intermolecular attractions between the PU segments[46, 57, 58]. The greater segmental motions in the polymer chains has occurred which in turn aid flexibility to PU backbone. The lowest T_g value is seen for 5wt% clay sample. It can be observed that with the addition of graphene along with the clay, T_g followed an increasing trend. The presence of graphene particles in the PU has certainly restricted the motions, but the dominance of clay layers in the matrix resulted in a lower T_g value when compared with neat PU.

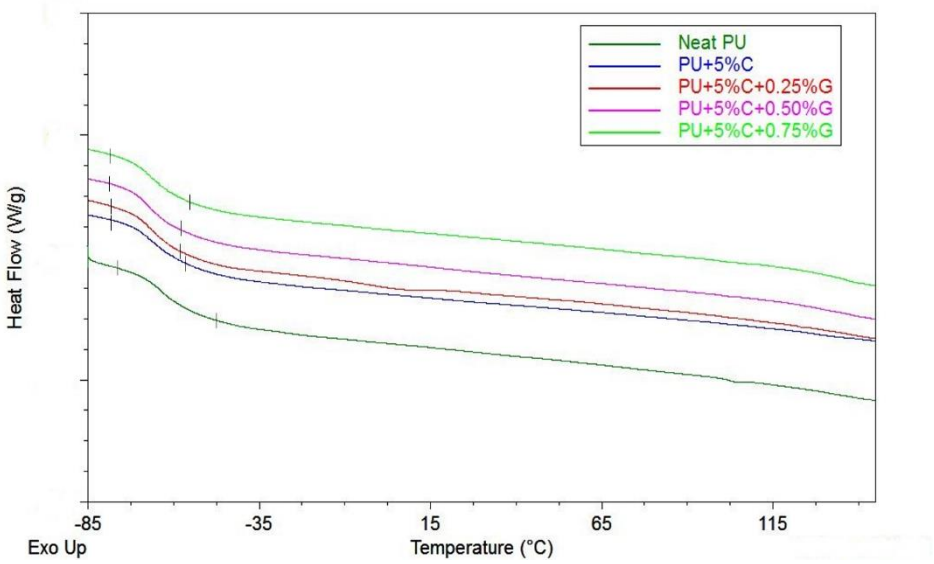

Figure 13 DSC plot of dual-additive PU composites at higher loadings of clay

The nanocomposites are exposed to liquid nitrogen temperature for 2 hours and allowed to come back to room temperature. These samples are tested to analyze the effect of cryogenic exposure. The below figures depict the dependence of T_g on sudden changes in temperature. A small change in T_g is observed which is because of the change in free volume due to unexpected changes in temperatures. It can also be expected that the polymer chains might have locked at a certain degree of freedom during the process culminating to an incomplete reversibility of molecular motions

therefore diminishing the chain flexibility. The glass transition temperatures of all the specimens before and after cryogenic exposure are shown in the table1.

A 2% increase in T_g was noticed in neat polyurethane and single-additive composites after dipping in liquid nitrogen. The additives clay, graphene and their weight concentrations do not seem to effect T_g with cryogenic exposure as the deviation is much like neat polyurethane. The neat polyurethane sample is expected to undergo a higher change in free volume because of thermal contraction and expansion that occur during the process. In the composites, large surface area and rigid nature of the additives would restrict this effect by a minimal change in free volume. However, the dual-additive composites at 1wt% and higher loadings of clay also shown a variation of around 2% in T_g except the composites with 5%C+0.5%G and 5%C+0.75%G which raised T_g by 3.6% and 3.07% respectively. Overall, two hours of cryogenic exposure did not make a significant change in the glass transition temperature hinting the suitability of PU for cryogenic applications.

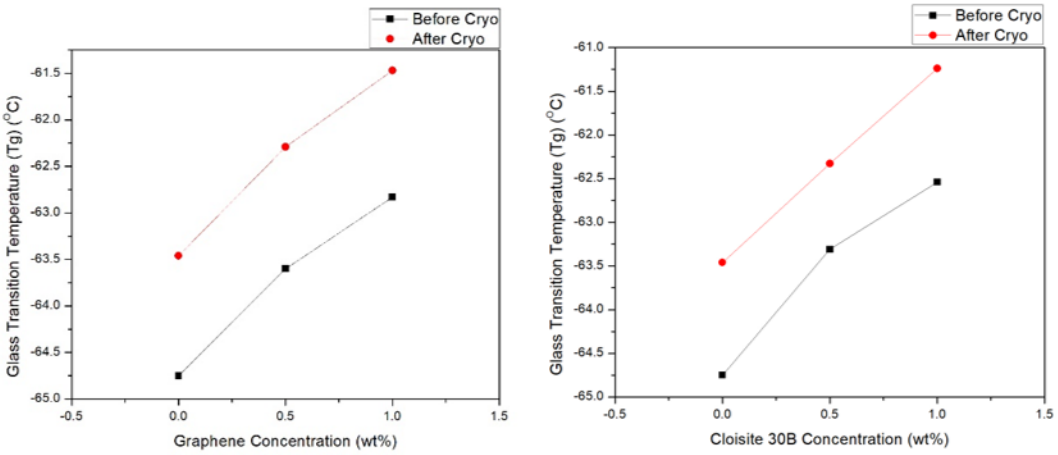

Figure 14 T_g variation in single-additive PU composites before and after cryogenic exposure

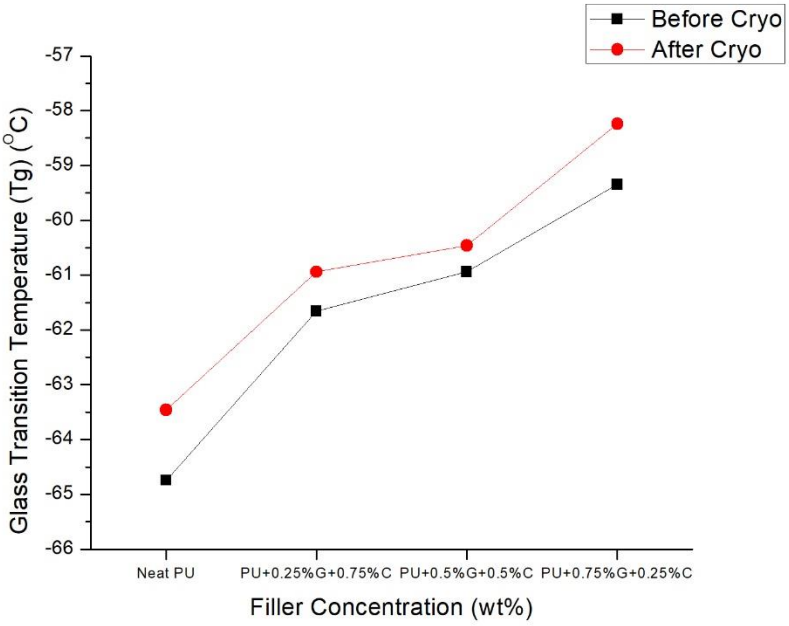

Figure 15 T_g variation in dual-additive PU composites at 1wt% before and after cryogenic exposure

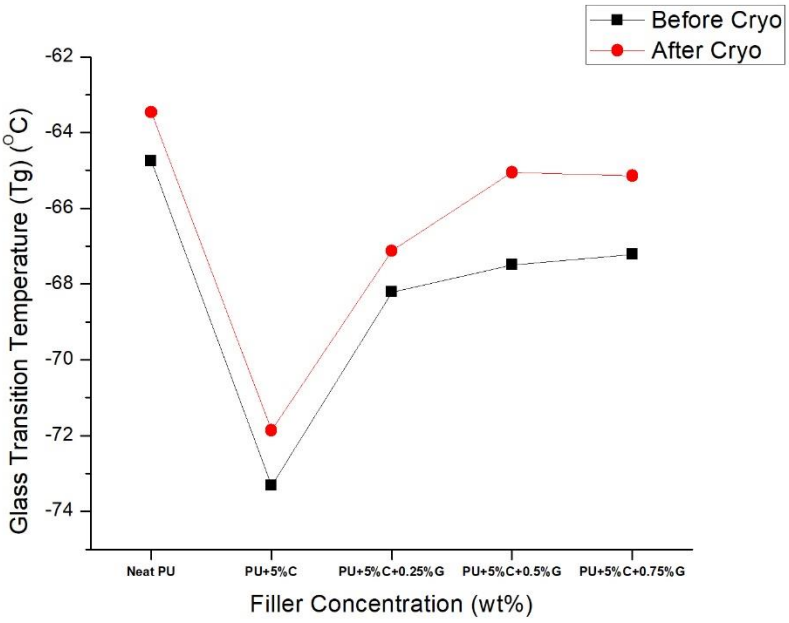

Figure 16 T_g variation in dual-additive PU composites at higher loadings of clay before and after cryogenic exposure

Table1 Glass Transition Temperature of polyurethane and its composites before and after cryogenic exposure

COMPOSITION	GLASS TRANSITION TEMPERATURE (T_g) (^{0}C)	
	BEFORE CRYO	AFTER CRYO
Neat PU	-64.75	-63.46
PU+0.5%C	-63.31	-62.23
PU+0.5%G	-63.60	-62.29
PU+1%C	-62.54	-61.24
PU+1%G	-62.83	-61.47
PU+0.25%G+0.75%C	-61.66	-60.94
PU+0.50%G+0.50%C	-60.94	-60.46
PU+0.75%G+0.25%C	-59.35	-58.24
PU+5%C	-73.32	-71.86
PU+5%C+0.25%G	-68.21	-67.12
PU+5%C+0.50%G	-67.49	-65.05
PU+5%C+0.75%G	-67.21	-65.14

3.2 Surface Morphology

SEM was used to understand the dispersion of nano-additives with the polyurethane matrix. It can be observed from below images that both the additives have mixed properly with the matrix. The graphene dispersion in the soft segment obtained from Applied graphene and the clay mixed with the hard segment has bonded very well at 0.5wt% and 1wt% loadings. Due to chemical affinity of these fillers with the matrix, they are very well interconnected leading to a uniform dispersion. A strong interphase is created between the fillers and matrix, which is necessary in enhancing the

properties of nanocomposites. There was no evidence of any kind of agglomerations or particle separation from the matrix. However, some air bubbles were seen in some samples which might have formed while pouring the blend into the mold. The specimens with both the additives together have also shown no clumps of particles. As the additives are mixed in different phases of the matrix, initially they have dispersed uniformly within the phase and attributed to even distribution throughout the matrix. The clay content was raised to 5wt% and graphene content was varied below 1wt% to understand the properties at higher loadings of clay. However, increase in clay content has led to formation of aggregates. The clay particles were clustered together on the surfaces which may act as crack initiators and defects, leading to a reduction in some of the useful properties of the nanocomposites.

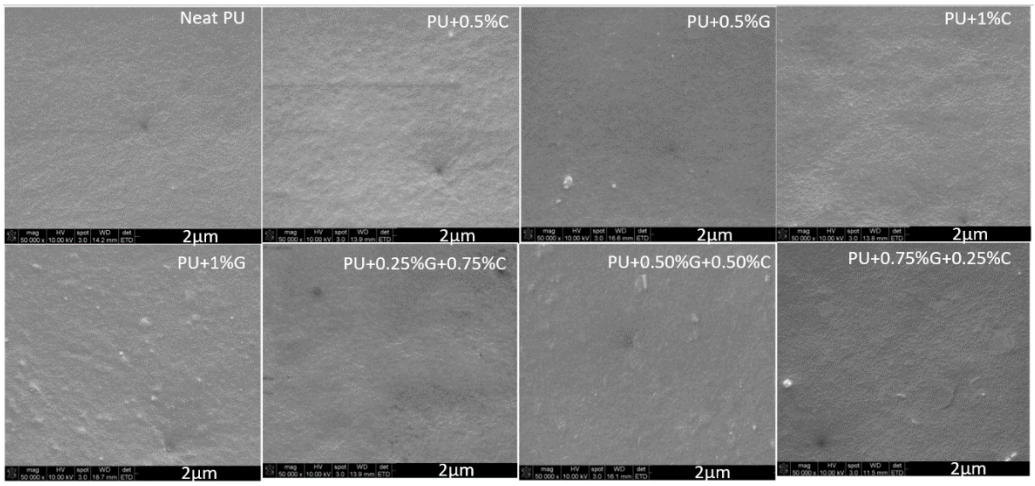

Figure 17 Surface images of Neat Polyurethane and its composites

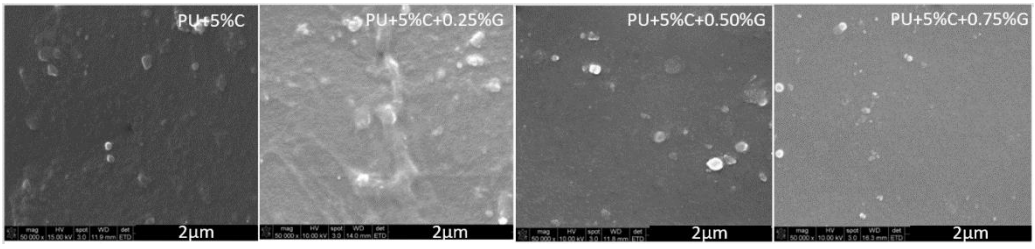

Figure 18 Surface images of Polyurethane composites at higher loadings of clay

The morphology of the fractured surfaces was determined after exposing the samples to liquid nitrogen temperature. The formation of microcracks in the neat polyurethane sample can be seen in the figure 19. This could be due to the brittleness of the material at liquid nitrogen temperature. At low temperatures, matrix becomes stiffer and stronger but less ductile. The internal stresses generated due to thermal contraction could lead to matrix failure by generating cracks. When the sample is dipped in liquid nitrogen, the external surface of the material starts to shrink while the internal core remains at room temperature with no contraction. The outer layers become rigid by the time internal core begin to contract dawning to thermal residual stresses. This residual stress occurs twice in the same sample due to sudden changes in the temperature from room temperature (RT) to cryogenic temperature (CT) and vice versa. When these stresses in the material become large enough they are relieved through physical processes such as microcracking. This effect of thermal shock can be minimized by toughening the material with nano-additives. The samples with graphene and clay at loadings below 1wt% showed resistance to the cracks because of the good dispersion. This can be explained for graphene and clay as the embedment of PU matrix within the layers and acting as stacking agents in crack propagation. The resistance to microcracking can be achieved by controlled addition of nano-fillers in the PU matrix which act as bridges to crack initiation and propagation due to abrupt changes in temperature.

The specimens with higher loadings of clay suggested that the cracks not only initiated at the agglomerates but also propagated through these clumps. These agglomerates act as crack initiators at low temperatures as the matrix shrinks. Due to this thermal mismatch, debonding occurs at the interface accelerating the crack formation. This is in accordance with the glass transition results. The decrease in T_g values is because of the backbone flexibility caused by the existence of agglomerates and diminishing the ability of PU to accommodate thermal stresses and intermolecular attractions. The toughness of the material decreases due to embrittlement and

molecular motions at low temperatures lowering the strength. Moreover, these cracks can also act as leaking pathways for the gas augmenting the permeation.

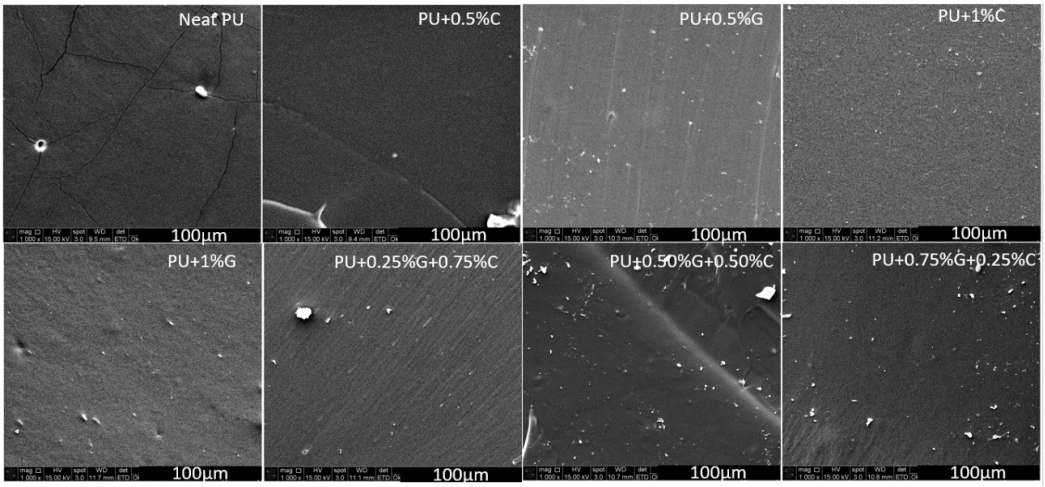

Figure 19 Surface images of neat polyurethane and its composites after cryogenic exposure

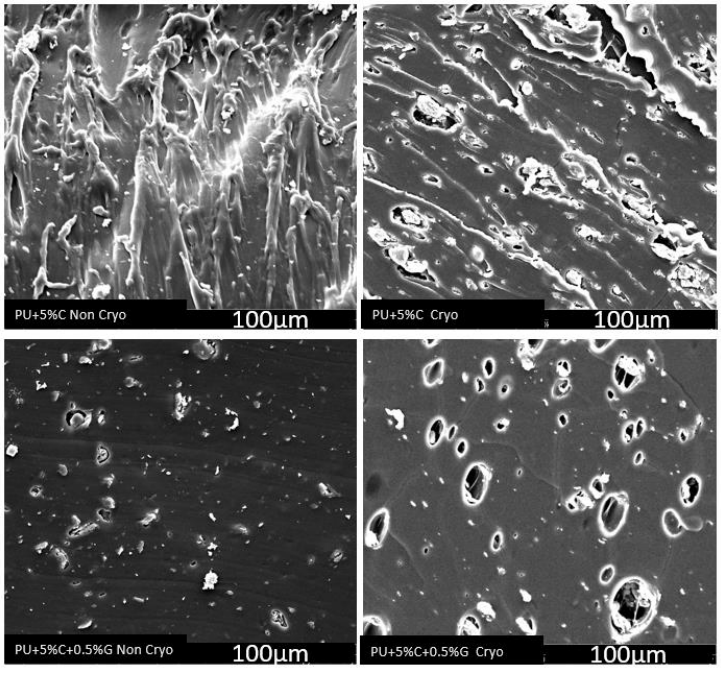

Figure 20 Surface images of polyurethane composites at higher loadings of clay before and after cryogenic exposure

3.3 Viscoelastic Properties

The viscoelastic properties of the polyurethane and its composites are obtained from DMA. The changes in molecular relaxations and modulus of the material at different temperatures and frequencies can be understood using this analysis. The storage modulus (E') provides a measure of elastic energy stored in a material during a cycle of sinusoidal deformation. The dependence of storage modulus on temperature and the filler concentrations is plotted in below figures. The inset figures indicates the storage modulus variation from 0^0C to 40^0C. It is evident from the graph that the storage modulus decreases with an increase in temperature from -100^0C to 50^0C denoting that the material is stiffer at low temperatures. A sharp drop down in the modulus values can be seen in the temperature range -70^0C to -40^0C due to transition of the material from glassy state to rubbery state. Molecular motions are restricted by addition of fillers, therefore increasing the stiffness. The storage modulus values of all the composites are higher when compared with the neat polyurethane and maintained consistency with DSC and SEM results. The proper dispersion of nano-additives in the polyurethane matrix improved glass transition temperature, therefore enhancing the stiffness. The graphene samples exhibited better modulus than clay samples as they are very well dispersed in soft phase. The rise in modulus at -100^0C is 6% and 16.3% for 0.5wt% of clay and graphene respectively when compared with neat polyurethane and a further increase to 21.6% and 26.3% with 1wt% loadings was observed.

The specimens with dual-additives at 1wt% loadings have shown a greater modulus values when compared with the individual filler loadings. The proximity of different material constituents in these composites aided in storing more elastic energy. The variation in graphene content from 0.25wt%, 0.5wt% and 0.75wt% in the soft phase of the matrix boosted the storage modulus. The higher the clay content, lower the storage modulus of the composite. This can be elucidated from the interaction of clay and graphene with soft phase of the matrix. As discussed earlier, elastic nature of the polyurethane relies on the soft phase and graphene is highly dispersed in the soft phase

while clay has dispersed in the hard phase. This might have allowed the high graphene composites in becoming stiffer when compared. A significant increase of 26.3%, 50.4% and 49.82% of modulus was viewed in the dual-additive composites when related to neat polyurethane.

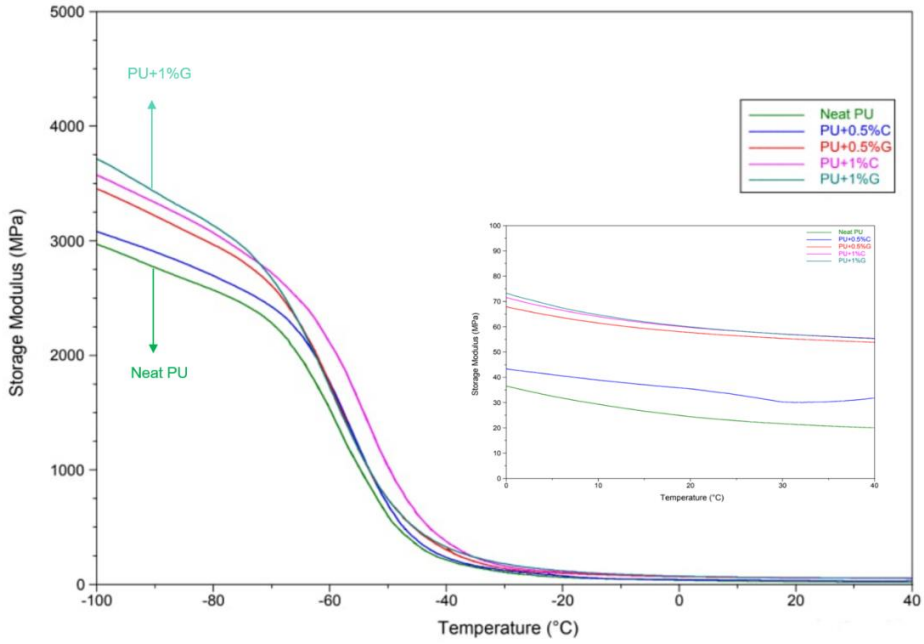

Figure 21 Storage modulus (E') plots of single-additive PU composites

The higher loadings of the clay didn't follow any trend at low temperatures. The 5wt% clay and the 5wt% clay+ 0.75wt% graphene composites appeared to have a modulus value equal to that of neat PU. This outcome is in consistence with the Tg values. The insertion of more amounts of clay into the matrix improved backbone flexibility and decreased the glass transition temperature. Hence, the material is more flexible than neat PU at lower temperatures in the Tg range. However, clay samples with the inclusion of graphene exhibited better stiffness above glass transition.

The neat polyurethane and its composites thin sheets are placed in liquid nitrogen filled Dewar for 2 hours. The samples are then allowed to come back to room temperature before testing. As discussed earlier, the storage modulus of the samples depends on molecular relaxations, which may

be affected due to sudden changes in temperature. The testing of the composites after cryogenic exposure would provide an idea on the mutation of the molecular relaxations.

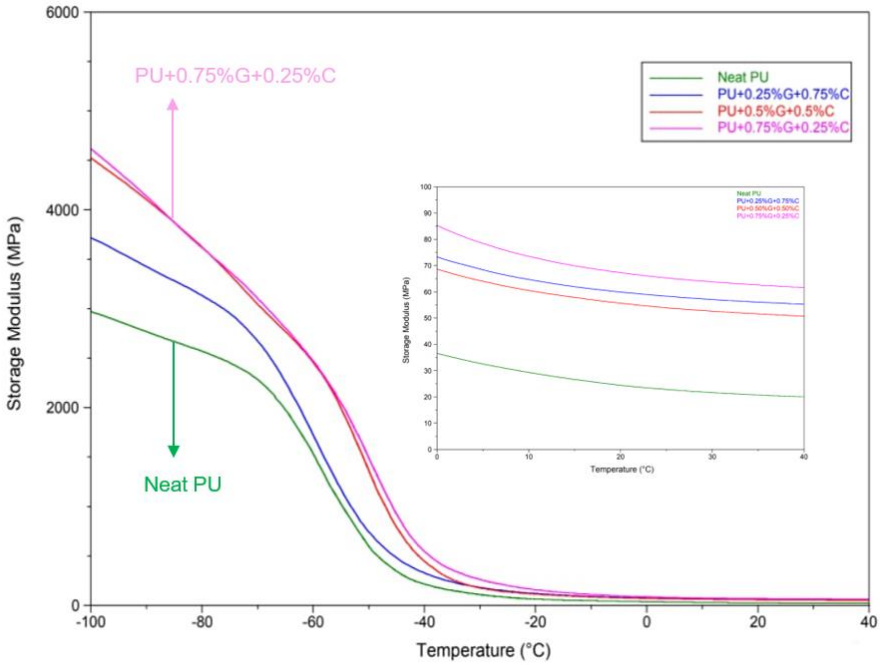

Figure 22 Storage modulus (E') plots of dual-additive PU composites at 1wt%

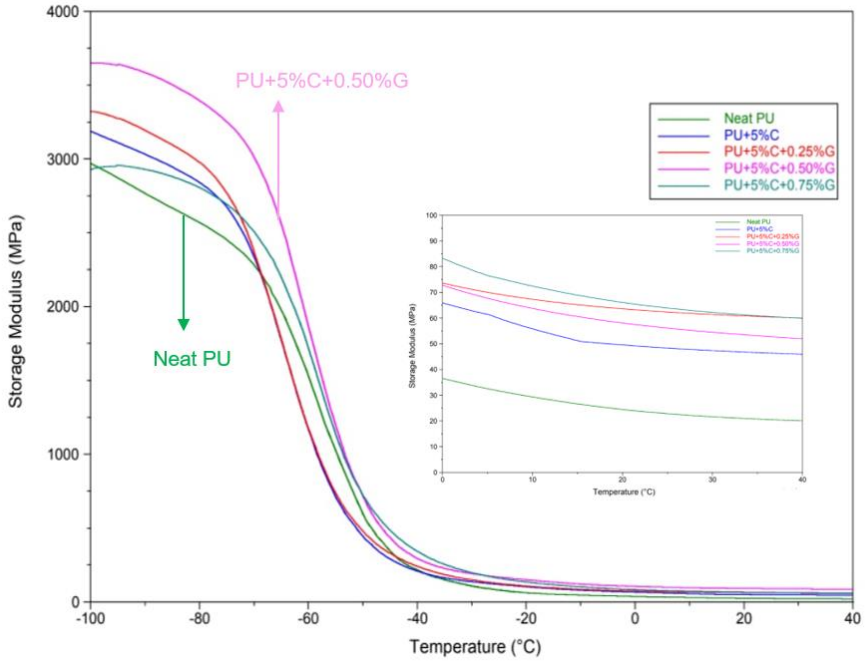

Figure 23 Storage Modulus (E') of dual-additive composites at higher loadings of clay

The storage modulus of the samples before and after cryogenic exposure are compared in the below figures. It was noticed that the modulus has been lowered in all the samples with cryogenic exposure. A minimum decrease of 4.5% and a maximum of 16.1% was seen in 0.5wt% graphene and 0.5wt% clay samples respectively, while the storage modulus in all the other compositions dropped was within 10% for one-additive composites. This can be explained as the clay was mixed initially with the hard phase, the cryogenic treatment of sample might have softened this phase by reducing the overall stiffness of the composite.

The composites with dual additives within 1wt% has suggested that the cryogenic treatment has no effect on the stiffness or storage modulus. The exposure has lowered the modulus less than 5% in all the three composites. The samples with 5wt% clay has also denoted around 10% change in modulus value at -100^{0}C. With the presence of graphene in the soft phase of the matrix, the modulus value has not changed significantly while the samples with 0.5wt% clay, 1wt% clay and 5wt% clay diminished the modulus by 16.1%, 8.9% and 9.1% respectively.

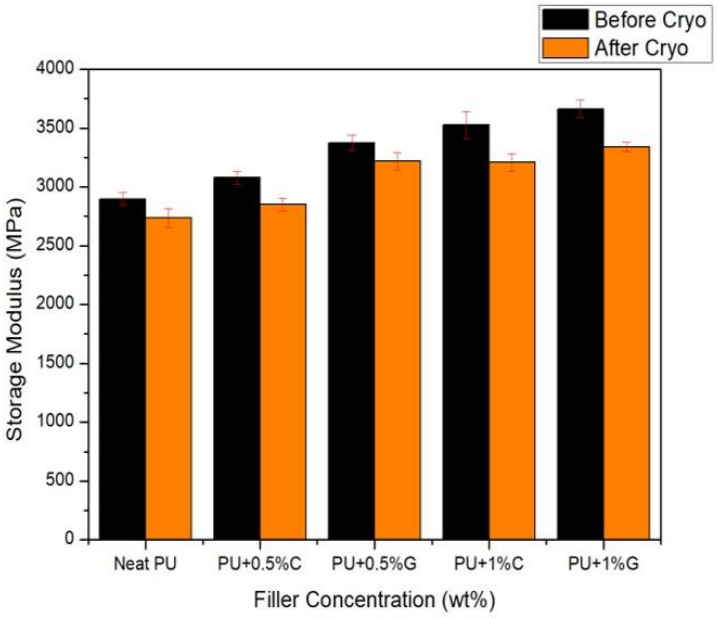

Figure 24 Bar chart showing storage modulus (E') variation at -100^{0}C in single-additive PU composites before and after cryogenic exposure

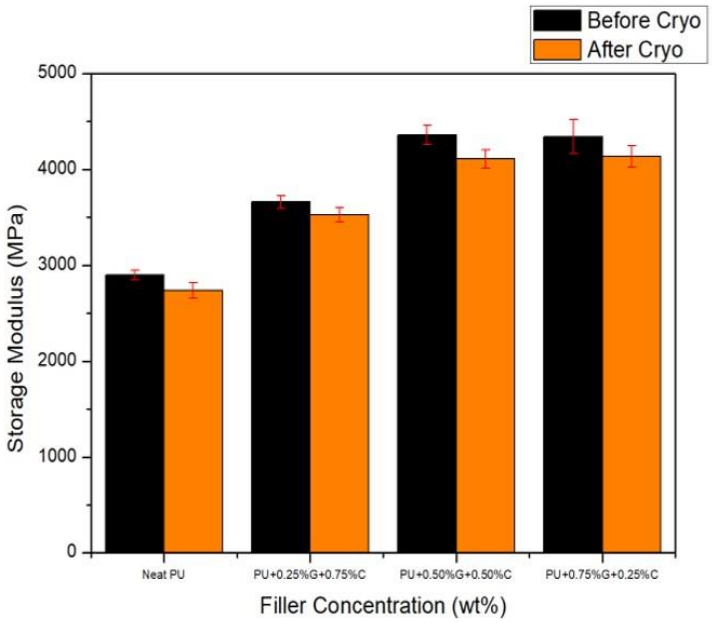

Figure 25 Bar chart showing storage modulus (E') variation at -100^{0}C in dual-additive PU composites at 1wt% before and after cryogenic exposure

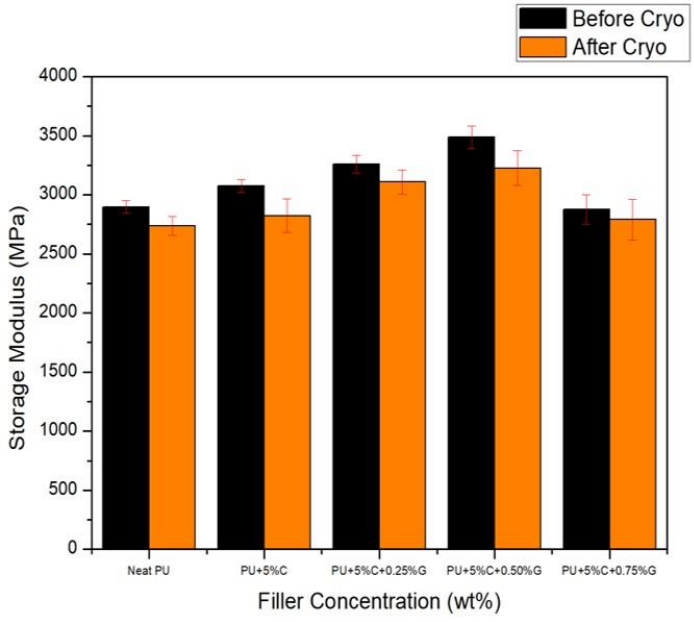

Figure 26 Bar chart showing storage (E') modulus variation at -100^{0}C in dual-additive PU composites at higher loadings of clay before and after cryogenic exposure

Table 2 Storage Modulus (E') at -100^{0}C of polyurethane and its composites before and after cryogenic exposure

COMPOSITION	STORAGE MODULUS (E') (MPa)	
	BEFORE CRYO	AFTER CRYO
Neat PU	2898±52.37	2736±78.99
PU+0.5%C	3077.4±52.23	2850.8±55.87
PU+0.5%G	3372.2±65.27	3220.2±73.94
PU+1%C	3525.6±114.24	3210.6±74.15
PU+1%G	3662.6±71.83	3337.6±39.92
PU+0.25%G+0.75%C	3661.8±66.17	3526.2±74.73
PU+0.50%G+0.50%C	4359.8±96.95	4107.6±95.39
PU+0.75%G+0.25%C	4342.8±176.84	4135.4±112.47
PU+5%C	3074.6±56.15	2823.2±141.85
PU+5%C+0.25%G	3259±74.69	3107.8±102.54
PU+5%C+0.50%G	3487±96.24	3225.2±148.10
PU+5%C+0.75%G	2875.2±123.75	2789.2±171.76

The stress strain analysis at different temperatures was carried out in DMA. A force of 18N was applied in tensile mode for all the samples. It was noticed that the thermal contraction is occurring in the material even at 0^{0}C, just below the room temperature for neat Polyurethane. As the temperature goes further down, the contraction of the sample has increased. There was no positive strain in the sample below the glass transition temperature i.e., at -70^{0}C. Though same force is applied at all temperatures, the applied force was not sufficient to stretch the sample at very low temperatures.

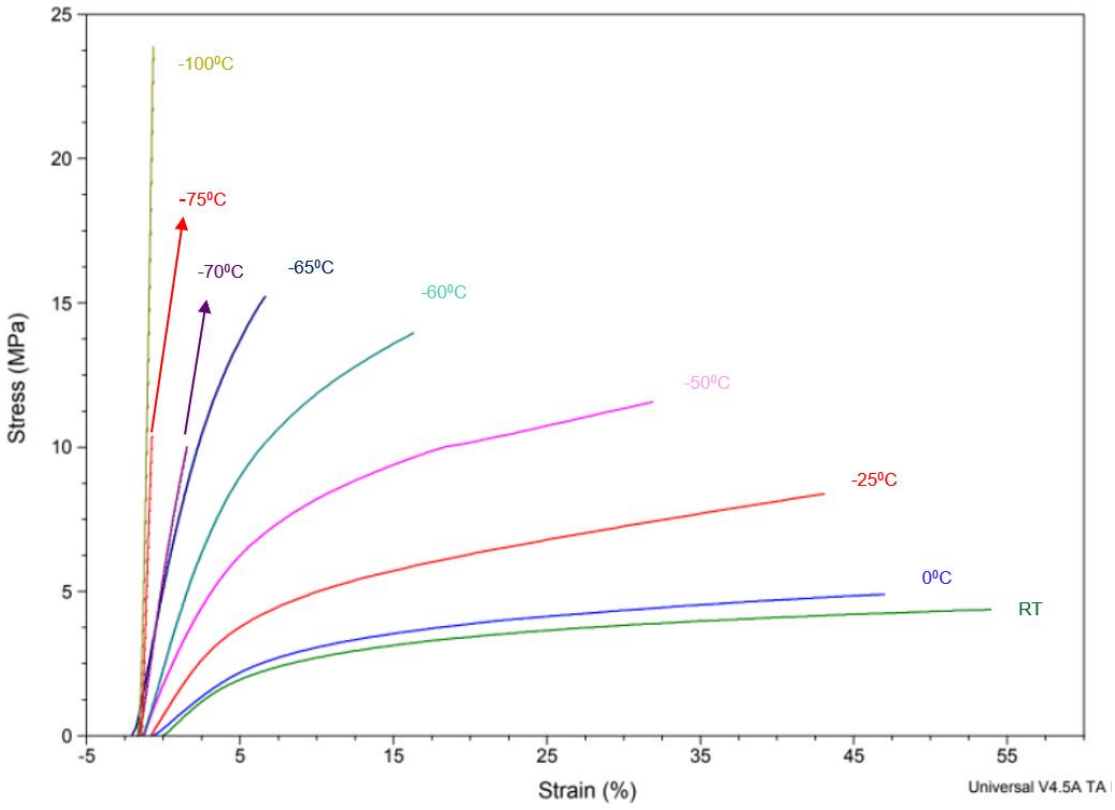

Figure 27 Stress-Strain diagram of neat polyurethane at different temperatures

3.4 Tensile Properties

The tensile modulus (E) and tensile strength of the composites are obtained from Instron machine. The tensile strength of the samples with low loadings of graphene and clay was not clearly understood as the Instron's movable gauge has reached its roof position. The tensile modulus of all the samples was calculated from the slope of the stress-strain curve. The modulus is enhanced by a minimum of 6% to maximum of 13.5% in the one-additive composites. It was noticed that the graphene composites have attained better modulus values compared with the clay composites. This is due to addition of graphene to the soft phase which dominates most of the properties of the polyurethane. It can also be understood from law mixtures that by adding higher modulus nano-

fillers to polyurethane matrix, the tensile modulus of the composite would possibly higher than neat polyurethane. The stress strain behavior of polyurethane composites is shown in the below figures. The inset figures represent the behavior at lower strains and the arrow indicates that samples can elongate further before breaking.

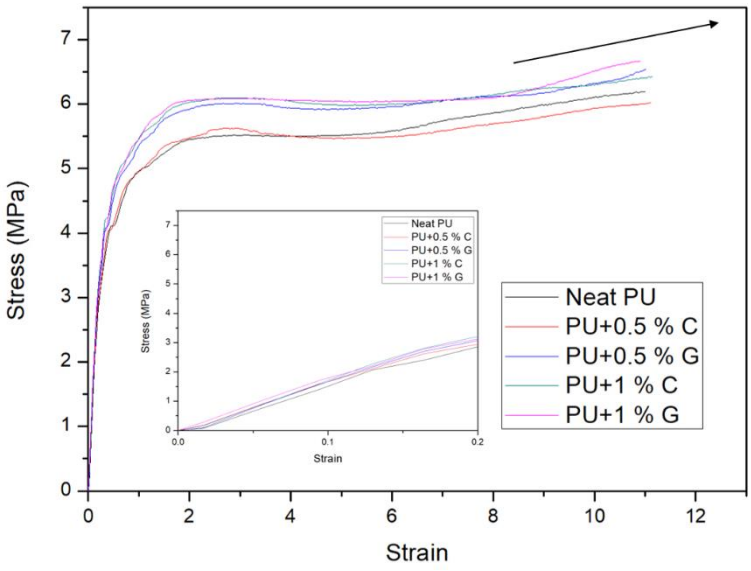

Figure 28 *Stress-Strain plot of single-additive PU composites*

The dual-additives composites have further increased the modulus of polyurethane confirming the glass transition and stiffness results. An increase of around 52% in the modulus was observed for PU+0.5%G+0.5%C composite. This can be explained by strong interfacial interaction of clay with hard domain and graphene with soft domain of polyurethane matrix. It should to be noted that for all the composites with two-additives, the modulus values are higher than the 1wt% loadings of the one-additive composites.

The stress-strain curve of composites with 5% clay is displayed in the figure 30. Unlike the neat polyurethane and lower loading composites, these samples broke at testing conditions signifying the reduction in tensile strength. The clay agglomerations formed at these loadings have attributed to the breaking of the samples at low stress when compared with other composites. The tensile

modulus is also lessened by adding higher contents of clay while the graphene addition to the composites has raised the modulus value. This result is also consistent with the decreased glass transition values by the addition of clay at 5wt%.

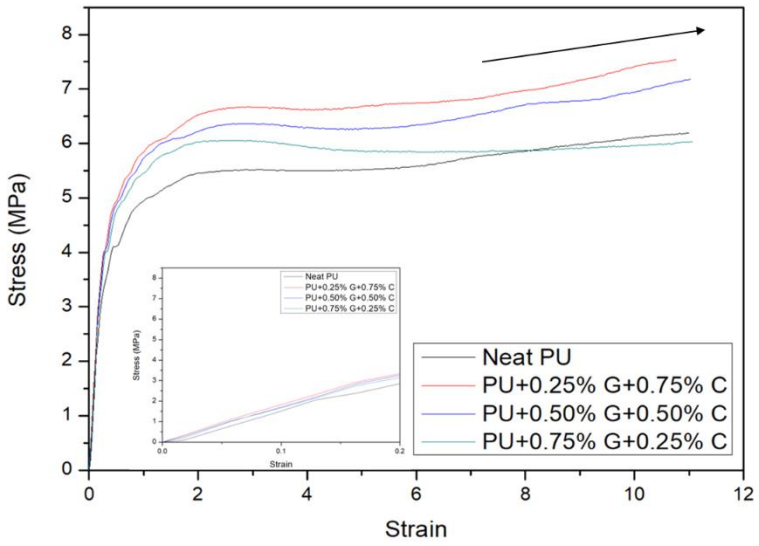

Figure 29 Stress-Strain plot of dual-additive PU composites at 1wt%

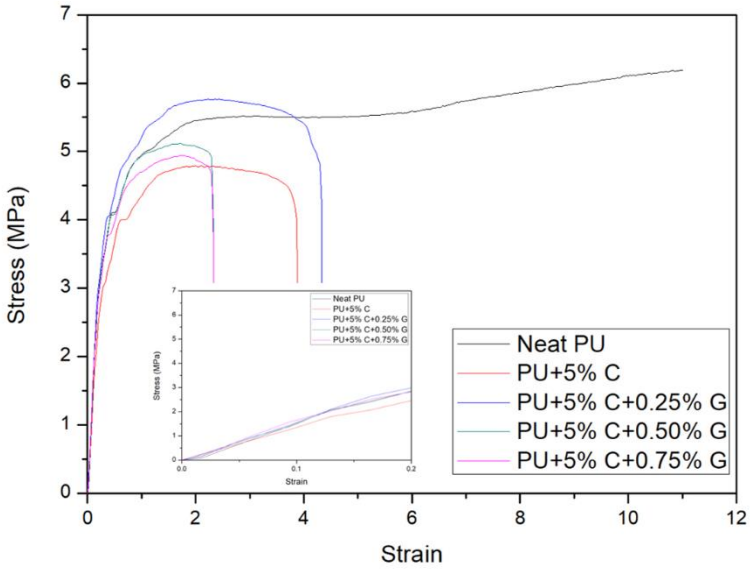

Figure 30 Stress-Strain plot of dual-additive PU composites at higher loadings of clay

The tensile modulus and strength of the composites are measured after exposing to cryogenic temperatures. The neat polyurethane and composites with clay has suffered a loss of 15% or more in modulus while the graphene samples experienced a loss of 10% in the modulus. The decrease in modulus might be because of the softening effect of clay on the hard domain allowing it to deform more easily. The thermal contraction of the sample during cryogenic exposure might have affected the crosslinks in the polymer network.

In the dual-additive composites no considerable change was seen in the tensile modulus with cryogenic exposure. A decrease of 5% and 2% were observed in PU+0.25%G+0.75%C and PU+0.5%G+0.5%C composites while an increase of 5% was observed in PU+0.75%G+0.25%C composite. This indicates that the filling of hard and soft domains with different fillers unalter the modulus of the composite after cryogenic exposure.

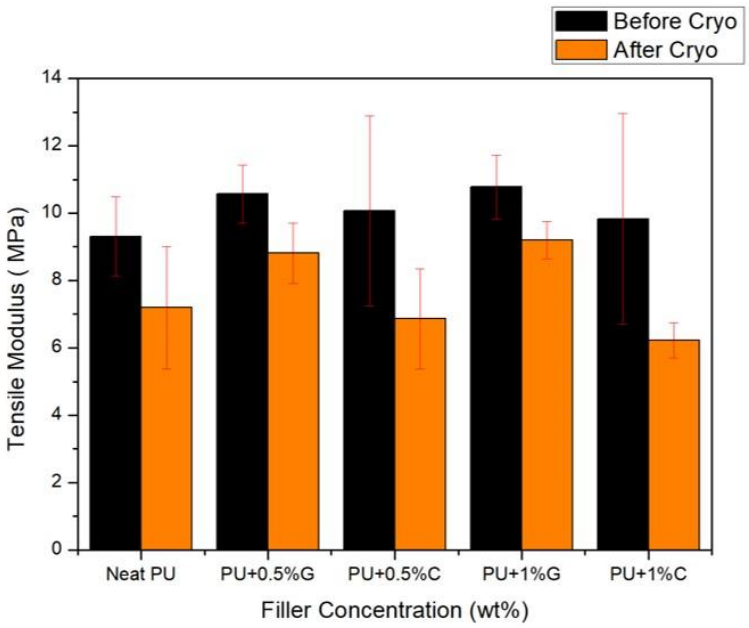

Figure 31 Bar Chart showing tensile modulus (E) variation in single-additive PU composites before and after cryogenic exposure

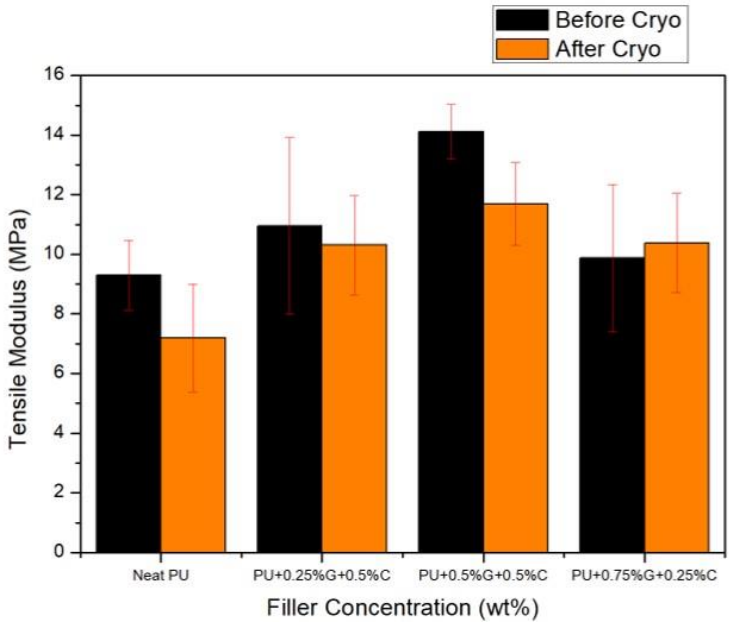

Figure 32 Bar Chart showing tensile modulus (E) variation in dual-additive PU composites at 1wt% before and after cryogenic exposure

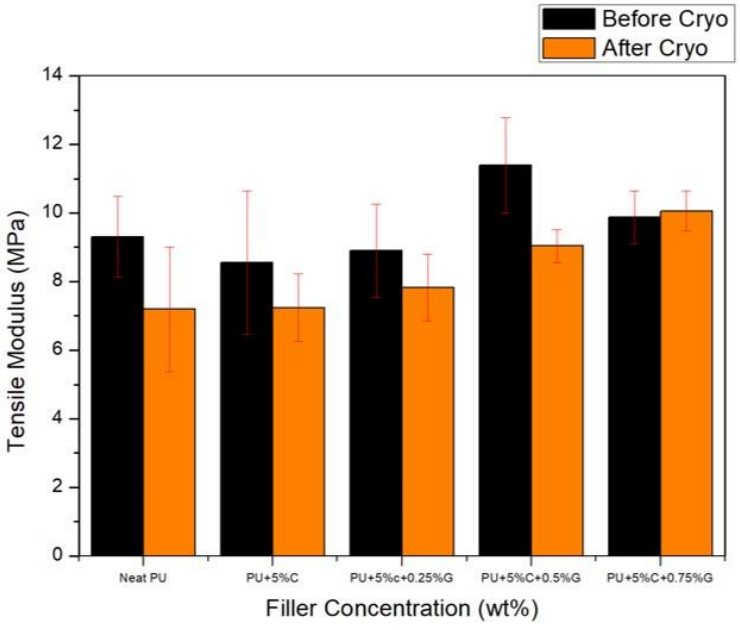

Figure 33 Bar Chart showing tensile modulus (E) variation in dual-additive PU composites at higher loadings of clay before and after cryogenic exposure

The composites with higher loadings of clay behaved much like the one-additive composites by decreasing the modulus around 15% for 5% clay, 11% for PU+5%C+0.25%G, 7% for PU+5%C+0.5%G. But interestingly a 2% increase in modulus was observed in PU+5%C+0.75%G. Moreover, a decrease in tensile strength of the composite at these concentrations is expected because of the cracks formation with cryogenic treatment which act as defects and break the sample at much lower stress.

Table 3 Tensile Modulus of polyurethane and its composites before and after cryogenic exposure

COMPOSITION	TENSILE MODULUS (E) (MPa)	
	BEFORE CRYO	AFTER CRYO
Neat PU	9.30±1.31	7.19±2.02
PU+0.5%C	10.06±3.15	6.86±1.66
PU+0.5%G	10.56±0.96	8.81±0.99
PU+1%C	9.83±3.49	6.22±0.59
PU+1%G	10.77±1.05	9.19±0.62
PU+0.25%G+0.75%C	10.95±2.96	10.31±1.65
PU+0.50%G+0.50%C	14.11±0.91	11.69±1.39
PU+0.75%G+0.25%C	9.87±2.47	10.37±1.67
PU+5%C	8.56±2.08	7.23±0.98
PU+5%C+0.25%G	8.90±1.35	7.82±0.97
PU+5%C+0.50%G	11.38±1.38	9.03±0.47
PU+5%C+0.75%G	9.88±0.76	10.06±0.57

The tensile strength of the dual-additive composites at higher loadings is listed in table-4. Initially the strength of the composites is increased with increasing graphene content because of the effective load transfer between the matrix and graphene. An increase of 8%, 12.15% and 12.74% of strength was observed in PU+5%C+0.25%G, PU+5%C+0.50%G and PU+5%C+0.75%G respectively when compared with PU+5%C. At the same time, the cryogenic exposure has dropped the strength in all the composites. This is predictable as microcracks were observed in SEM for all these composites. But, these cracks do not appear to have a large impact on the strength because only 3%, 3%, 8.3% and 5.9% of reduction in strength was noticed.

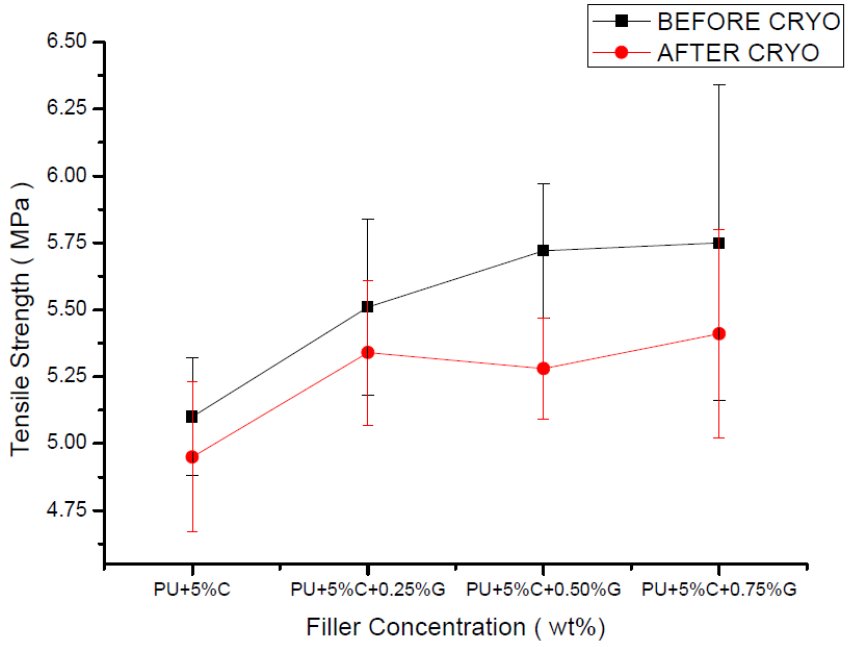

Figure 34 Tensile Strength variation in dual-additive PU composites at higher loadings of clay before and after cryogenic exposure

Table 4 Tensile Strength of dual-additive composites at higher loadings of clay before and after cryogenic exposure

COMPOSITION	TENSILE STRENGTH (MPa)	
	BEFORE CRYO	AFTER CRYO
PU+5%C	5.10±0.22	4.95±0.28
PU+5%C+0.25%G	5.51±0.33	5.34±0.27
PU+5%C+0.50%G	5.72±0.25	5.28±0.19
PU+5%C+0.75%G	5.75±0.59	5.41±0.39

CHAPTER IV

CONCLUSIONS

Polyurethane nanocomposites with graphene and cloisite 30B as fillers are prepared and the properties are analyzed. The composites with dual additives have shown a better improvement in T_g, stiffness and modulus than the single additive composites at equal concentrations. The presence of graphene has raised the T_g while the clay at higher loadings (5wt%) has decreased the T_g by affecting the intermolecular interactions between hard phase and soft phase. The surfaces of the composites suggested that both the additives dispersed uniformly in the matrix except the 5wt% clay composites, where some agglomerates were seen, which eventually led to microcracking when exposed to cryogenic liquids. The stiffness of the composites at -100^0C increased with an increase in filler concentration and the dual-additive composites were stiffer than single-additive composites at similar loadings, however the stiffness was reduced by less than 10% in most of the composites after cryogenic exposure. The tensile testing of the composites implied an enhancement in the tensile modulus with addition of fillers, a 50% improvement in tensile modulus was seen in dual-additive PU composite with 0.5wt% graphene and 0.5wt% clay. Despite that, the cryogenic treatment of composites has degraded the modulus by 10% or more except for the dual-additive specimens at 1wt% concentrations. The tensile strength of the high clay content dual-additive composites increased with graphene addition, dropped with cryogenic exposure due to microcrack formation. This study suggested that polyurethane composites could be suitable materials for cryogenic applications. Nevertheless, there are many other factors like CTE, prolonged exposure

time, layer delamination, permeability and other mechanical properties which needs to be investigated prior to making a conclusion.

CHAPTER V

FUTURE WORK

The composites will be examined in FTIR and XRD to understand more about the nature of clay and graphene in dual-additive composites. These experiments might provide a possible approach to analyze clay-graphene interactions in the polymer network. Future work will also focus on measuring the coefficient of thermal expansion and permeability of the composites with and without cryogenic exposure. The prolonged exposure to liquid nitrogen would be attained by implementing the thermal cycling process on composites. In each cycle, the composites remain at cryogenic and room temperatures for equal times. The mechanical testing of composites at cryogenic temperature would suggest better understanding of the material behavior at low temperatures.

REFERENCES

1. Coopersmith, J., *The cost of reaching orbit: Ground-based launch systems.* Space Policy, 2011. **27**(2): p. 77-80.
2. Lamoreaux, A.J., *Final Report on Audit of Space Launch Initiative : Primary Requirements for A 2nd Generation Reusable Launch Vehicle*, R.N. IG-02-028, Editor. 2002, Office of Inspector General, The National Aeronautics and Space Administration,Washington, DC, USA.
3. Chen, Q.-S., J. Wegrzyn, and V. Prasad, *Analysis of temperature and pressure changes in liquefied natural gas (LNG) cryogenic tanks.* Cryogenics, 2004. **44**(10): p. 701-709.
4. CTD, Next Generation Pressure Vessels, Composite world news, available at *https://www.compositesworld.com/articles/next-generation-pressure-vessels*. 2012.
5. Tracy McMahan, J.A., " Move Over Heavy Metal, There is a New Tank Coming to Town". *https://www.nasa.gov/centers/marshall/news/news/releases/2014/14-043.html*. 2014.
6. Tapeinos, I.G. and S. Koussios, *Experimental study on various liner materials for cryogenic liquid hydrogen storage*. 2013, Materials.
7. Maganty, S., et al., *Enhanced mechanical properties of polyurethane composite coatings through nanosilica addition.* Progress in Organic Coatings, 2016. **90**: p. 243-251.
8. Chattopadhyay, D.K. and K. Raju, *Structural engineering of polyurethane coatings for high performance applications.* Progress in polymer science, 2007. **32**(3): p. 352-418.
9. Rafiee, Z. and V. Keshavarz, *Synthesis and characterization of polyurethane/microcrystalline cellulose bionanocomposites.* Progress in Organic Coatings, 2015. **86**: p. 190-193.

10. Zia, K.M., et al., *Synthesis and molecular characterization of chitosan based polyurethane elastomers using aromatic diisocyanate.* International journal of biological macromolecules, 2014. **66**: p. 26-32.
11. Prisacariu, C., *Polyurethane Elastomers , from morphology to mechanical aspects*. 1 ed. 2011, Springer-Verlag Wien: Springer-Verlag Wien.
12. Szycher, M., *Szycher's handbook of polyurethanes*. 1999: CRC press.
13. North America Polyurethane Market Analysis , Grand View Research, available at *https://www.grandviewresearch.com/industry-analysis/north-america-polyurethane-market*. 2016.
14. Rajput, S.D., et al., *Fatty acids based transparent polyurethane films and coatings.* Progress in Organic Coatings, 2014. **77**(9): p. 1360-1368.
15. Akindoyo, J.O., et al., *Polyurethane types, synthesis and applications–a review.* RSC Advances, 2016. **6**(115): p. 114453-114482.
16. D16-16, A., *Standard Terminology for Paints, Related Coatings, Materials and Applications.* ASTM International, 2016.
17. Novoselov, K.S., et al., *Electric field effect in atomically thin carbon films.* science, 2004. **306**(5696): p. 666-669.
18. Tong, Y., S. Bohm, and M. Song, *Graphene based materials and their composites as coatings.* Austin Journal of Nanomedicine & Nanotechnology, 2013. **1**(1): p. 1003.
19. Singh, V., et al., *Graphene based materials: past, present and future.* Progress in materials science, 2011. **56**(8): p. 1178-1271.
20. Liao, K.-H., Y. Qian, and C.W. Macosko, *Ultralow percolation graphene/polyurethane acrylate nanocomposites.* Polymer, 2012. **53**(17): p. 3756-3761.
21. Alexander, *The ideal Crystalline structure of graphene is a hexagonal grid, available at https://commons.wikimedia.org/wiki/File:Graphen.jpg*,Wikimedia Commons, 2012.
22. Ray, S.S. and M. Okamoto, *Polymer/layered silicate nanocomposites: a review from preparation to processing.* Progress in polymer science, 2003. **28**(11): p. 1539-1641.

23. Giannelis, E.P., *Polymer-layered silicate nanocomposites: synthesis, properties and applications.* 1998.
24. Ogasawara, T., et al., *Helium gas permeability of montmorillonite/epoxy nanocomposites.* Composites Part A: Applied Science and Manufacturing, 2006. **37**(12): p. 2236-2240.
25. Bharadwaj, R.K., *Modeling the barrier properties of polymer-layered silicate nanocomposites.* Macromolecules, 2001. **34**(26): p. 9189-9192.
26. Feldman, D., *Polymer nanocomposite barriers.* Journal of Macromolecular Science, Part A, 2013. **50**(4): p. 441-448.
27. Yoo, B.M., et al., *Graphene and graphene oxide and their uses in barrier polymers.* Journal of Applied Polymer Science, 2014. **131**(1).
28. Dai, C.-F., P.-R. Li, and J.-M. Yeh, *Comparative studies for the effect of intercalating agent on the physical properties of epoxy resin-clay based nanocomposite materials.* European Polymer Journal, 2008. **44**(8): p. 2439-2447.
29. De Paiva, L.B., A.R. Morales, and F.R.V. Díaz, *Organoclays: properties, preparation and applications.* Applied clay science, 2008. **42**(1-2): p. 8-24.
30. Kalia, S. and S.-Y. Fu, *Polymers at cryogenic temperatures*. 2013: Springer.
31. Noh, J. and J. Whitcomb, *Effect of laminate design and loads on crack opening volume in laminates used in cryogenic tanks.* Journal of Composites, Technology and Research, 2003. **25**(3): p. 1-8.
32. Bechel, V.T. and R.Y. Kim, *Damage trends in cryogenically cycled carbon/polymer composites.* Composites science and technology, 2004. **64**(12): p. 1773-1784.
33. Bechel, V.T., J.D. Camping, and R.Y. Kim, *Cryogenic/elevated temperature cycling induced leakage paths in PMCs.* Composites Part B: Engineering, 2005. **36**(2): p. 171-182.
34. Bechel, V.T., et al., *Effect of stacking sequence on micro-cracking in a cryogenically cycled carbon/bismaleimide composite.* Composites Part A: Applied Science and Manufacturing, 2003. **34**(7): p. 663-672.

35. Bechel, V.T., M. Negilski, and J. James, *Limiting the permeability of composites for cryogenic applications.* Composites Science and Technology, 2006. **66**(13): p. 2284-2295.
36. Roy, S., A. Utturkar, and A. Nair. *Modeling and Characterization of Permeability and Damage Graphite/epoxy at Cryogenic Temperatures*. in *46th AIAA/ASME/ASCE/AHS/ASC Structures, Structural Dynamics and Materials Conference*. 2005.
37. Rivers, H.K., J.G. Sikora, and S.N. Sankaran, *Detection of hydrogen leakage in a composite sandwich structure at cryogenic temperature.* Journal of spacecraft and rockets, 2002. **39**(3): p. 452-459.
38. Kumazawa, H., T. Aoki, and I. Susuki, *Analysis and experiment of gas leakage through composite laminates for propellant tanks.* AIAA journal, 2003. **41**(10): p. 2037-2044.
39. Bechel, V. *Helium flow through cryogenically pre-conditioned composite laminates*. in *Proceedings of the 50th SAMPE international symposium, Long Beach, CA*. 2005.
40. Yokoeki, T., T. Aoki, and T. Ishikawa, *Experimental cryogenic gas leakage through damaged composite laminates for propellant tank application.* Journal of Spacecraft and rockets, 2005. **42**(2): p. 363-366.
41. Mallick, K., et al. *An integrated systematic approach to linerless composite tank development*. in *46th AIAA/ASME/ASCE/AHS/ASC Structures, Structural Dynamics and Materials Conference*. 2005.
42. Islam, M.S., et al., *Investigation of woven composites as potential cryogenic tank materials.* Cryogenics, 2015. **72**: p. 82-89.
43. Shen, X.-J., et al., *The reinforcing effect of graphene nanosheets on the cryogenic mechanical properties of epoxy resins.* Composites Science and Technology, 2012. **72**(13): p. 1581-1587.
44. Shen, X.-J., et al., *Improved cryogenic interlaminar shear strength of glass fabric/epoxy composites by graphene oxide.* Composites Part B: Engineering, 2015. **73**: p. 126-131.

45. Zhang, Y.-H., et al., *Studies on characterization and cryogenic mechanical properties of polyimide-layered silicate nanocomposite films.* Polymer, 2004. **45**(22): p. 7579-7587.
46. Yang, J.-P., et al., *Cryogenic mechanical behaviors of MMT/epoxy nanocomposites.* Composites Science and Technology, 2007. **67**(14): p. 2934-2940.
47. Miller, S. and M. Meador. *Polymer-layered silicate nanocomposites for cryotank applications*. in *48th AIAA/ASME/ASCE/AHS/ASC structures, structural dynamics, and materials conference*. 2007.
48. Gudarzi, M., et al. *Electrical and mechanical properties of polyurethane nanocomposites containing self-aligned graphene sheets*. in *ICCM International Conferences on Composite Materials*. 2011.
49. Cai, D., et al., *High performance polyurethane/functionalized graphene nanocomposites with improved mechanical and thermal properties.* Composites Science and Technology, 2012. **72**(6): p. 702-707.
50. Yadav, S.K. and J.W. Cho, *Functionalized graphene nanoplatelets for enhanced mechanical and thermal properties of polyurethane nanocomposites.* Applied surface science, 2013. **266**: p. 360-367.
51. Kim, H., Y. Miura, and C.W. Macosko, *Graphene/polyurethane nanocomposites for improved gas barrier and electrical conductivity*. Chemistry of Materials, 2010. **22**(11): p. 3441-3450.
52. Rahnama, M.R., et al., *An investigation into the effects of different nanoclays on polyurethane nanocomposites properties.* Polymer-Plastics Technology and Engineering, 2014. **53**(8): p. 801-810.
53. Cao, X., et al., *Polyurethane/clay nanocomposites foams: processing, structure and properties.* Polymer, 2005. **46**(3): p. 775-783.
54. Pattanayak, A. and S.C. Jana, *Synthesis of thermoplastic polyurethane nanocomposites of reactive nanoclay by bulk polymerization methods.* Polymer, 2005. **46**(10): p. 3275-3288.

55. Pattanayak, A. and S.C. Jana, *Thermoplastic polyurethane nanocomposites of reactive silicate clays: effects of soft segments on properties.* Polymer, 2005. **46**(14): p. 5183-5193.
56. Pattanayak, A. and S.C. Jana, *High-strength and low-stiffness composites of nanoclay-filled thermoplastic polyurethanes.* Polymer Engineering & Science, 2005. **45**(11): p. 1532-1539.
57. Seo, W., et al., *Synthesis and properties of polyurethane/clay nanocomposite by clay modified with polymeric methane diisocyanate.* Journal of applied polymer science, 2006. **101**(5): p. 2879-2883.
58. Zeng, Q., A. Yu, and G.M. Lu, *Interfacial interactions and structure of polyurethane intercalated nanocomposite.* Nanotechnology, 2005. **16**(12): p. 2757.

VITA

Vishanth Uppu

Candidate for the Degree of

Master of Science

Thesis: THE EFFECT OF NANOPARTICLES ADDITION ON THE PROPERTIES OF POLYURETHANE

Major Field: Materials Science and Engineering

Biographical:

Education:

Completed the requirements for the Master of Science in Materials Science and Engineering at Oklahoma State University, Tulsa, Oklahoma in May, 2018.

Completed the requirements for the Bachelor of Engineering in Mechanical Engineering at Osmania University, Hyderabad, Telangana, India in 2014.

Experience:

Graduate Research Assistant at Helmerich Research Center, Department of Materials Science and Engineering, Oklahoma State University, Tulsa, OK from August 2016 to May 2018.

Graduate Trainee at Center for Ceramic Processing, ARCI, Hyderabad, Telangana, India from February 2015 to February 2016.